Cancer Cell

CD44 Variant Regulates Redox Status in Cancer Cells by Stabilizing the xCT Subunit of System xc^- and Thereby Promotes Tumor Growth

Takatsugu Ishimoto,[1,3] Osamu Nagano,[1,2,*] Toshifumi Yae,[1] Mayumi Tamada,[1] Takeshi Motohara,[1] Hiroko Oshima,[4] Masanobu Oshima,[4] Tatsuya Ikeda,[5] Rika Asaba,[5] Hideki Yagi,[5] Takashi Masuko,[5] Takatsune Shimizu,[1,2] Tomoki Ishikawa,[1,6] Kazuharu Kai,[1] Eri Takahashi,[1] Yu Imamura,[3] Yoshifumi Baba,[3] Mitsuyo Ohmura,[7] Makoto Suematsu,[7,8] Hideo Baba,[3] and Hideyuki Saya[1,2]

[1]Division of Gene Regulation, Institute for Advanced Medical Research, School of Medicine, Keio University, 35 Shinanomachi, Shinjuku-ku, Tokyo 160-8582, Japan

[2]Core Research for Evolutional Science and Technology (CREST), Japan Science and Technology Agency, Tokyo160-8582, Japan

[3]Department of Gastroenterological Surgery, Graduate School of Medical Science, Kumamoto University, 1-1-1 Honjo, Kumamoto 860-8556, Japan

[4]Division of Genetics, Cancer Research Institute, Kanazawa University, 13-1 Takara-machi, Kanazawa 920-0934, Japan

[5]Cell Biology Laboratory, Department of Pharmaceutical Sciences, School of Pharmacy, Kinki University, 4-1 Kowakae 3-chome, Higashiosaka-shi, Osaka 577-8502, Japan

[6]Kasai R&D Center, Daiichi Sankyo Co. Ltd., 1-16-13 Kitakasai, Edogawa-ku, Tokyo 134-8630, Japan

[7]Department of Biochemistry, School of Medicine, Keio University, 35 Shinanomachi, Shinjuku-ku, Tokyo 160-8582, Japan

[8]ERATO Gas Biology Project, Japan Science and Technology Agency, Tokyo 160-8582, Japan

*Correspondence: osmna@sb3.so-net.ne.jp

DOI 10.1016/j.ccr.2011.01.038

SUMMARY

CD44 is an adhesion molecule expressed in cancer stem-like cells. Here, we show that a CD44 variant (CD44v) interacts with xCT, a glutamate-cystine transporter, and controls the intracellular level of reduced glutathione (GSH). Human gastrointestinal cancer cells with a high level of CD44 expression showed an enhanced capacity for GSH synthesis and defense against reactive oxygen species (ROS). Ablation of CD44 induced loss of xCT from the cell surface and suppressed tumor growth in a transgenic mouse model of gastric cancer. It also induced activation of $p38^{MAPK}$, a downstream target of ROS, and expression of the gene for the cell cycle inhibitor $p21^{CIP1/WAF1}$. These findings establish a function for CD44v in regulation of ROS defense and tumor growth.

INTRODUCTION

CD44, a major adhesion molecule for the extracellular matrix, has been implicated in a wide variety of physiological processes, including leukocyte homing and activation, wound healing, and cell migration, as well as in tumor cell invasion and metastasis (Gunthert et al., 1991; Nagano and Saya, 2004; Ponta et al., 2003). It exists in numerous isoforms generated through alternative mRNA splicing. Whereas the standard CD44 isoform (CD44s) is expressed predominantly in hematopoietic cells and normal epithelial cell subsets, variant isoforms (CD44v) with insertions in the membrane-proximal extracellular region are abundant in epithelial-type carcinomas (Tanabe et al., 1993). However, the functional relevance of CD44v in tumor cells remains unclear.

CD44 has recently been identified as one of the cell surface markers associated with cancer stem cells (CSCs) in several types of tumor (Al-Hajj et al., 2003; Collins et al., 2005; Dalerba

Significance

Cancer stem cells (CSCs) manifest enhanced protection against reactive oxygen species (ROS), rendering them resistant to chemo- or radiotherapy. Here, we show that expression of the CSC marker CD44, in particular that of a variant isoform (CD44v), contributes to ROS defense by promoting the synthesis of reduced glutathione (GSH), a primary intracellular antioxidant. CD44v interacts with and stabilizes xCT, a subunit of a glutamate-cystine transporter, and thereby promotes the uptake of cystine for GSH synthesis. Our findings reveal a role for CD44v in the protection of CSCs from high levels of ROS in the tumor microenvironment. Moreover, they provide a rationale for CD44v-targeted therapy to impair ROS defense in cancer cells and sensitize them to currently available treatments.

et al., 2007). CSCs are malignant cell subsets in hierarchically organized tumors; they are selectively capable of tumor initiation and self-renewal and give rise to the bulk population of nontumorigenic cancer cells through differentiation. Furthermore, we have recently shown that CD44v is heterogeneously expressed in mouse gastric tumors, being highly abundant in proliferative cells and slow-cycling stem-like cells, but not in cells harboring mucin 5AC (MUC5AC) mRNA, a marker of gastric differentiation (Ishimoto et al., 2010). These observations suggested that CD44 might play a role in tumor initiation and the maintenance of cancer cells in addition to its more established functions in cell adhesion and migration. However, function-based evidence to support such a role for CD44 or its variant isoforms has been lacking.

Oxidative stress occurs when production of reactive oxygen species (ROS) exceeds the capacity of the cellular defense system consisting of redox enzymes and other antioxidant molecules. Like normal tissue stem cells, subsets of CSCs in some tumors harbor only low levels of ROS and manifest enhanced mechanisms for protection against ROS-mediated damage, properties that may contribute to tumor resistance to chemo- and radiotherapy (Diehn et al., 2009; Phillips et al., 2006). Reduced glutathione (GSH) is a major cellular metabolite that protects against oxidative and chemical injury and exhibits a variety of other cytoprotective effects. High levels of GSH as well as increased expression of antioxidant enzymes promote cancer cell survival and resistance to anticancer agents (Trachootham et al., 2009). System xc^- is a cystine-glutamate exchange transporter composed of a light-chain subunit (xCT, SLC7A11) and a heavy-chain subunit (CD98hc, SLC3A2). Expression of xCT at the cell surface is essential for the uptake of cystine required for intracellular GSH synthesis and is, thus, an important determinant of intracellular redox balance (Lo et al., 2008). Cells deficient in xCT or depleted of GSH have recently been found to exhibit $p38^{MAPK}$ activation even at low levels of oxidative stress (Chen et al., 2009; Sato et al., 2005), indicating that xCT-mediated cystine transport for GSH synthesis plays a key role in prevention of such stress signaling. Furthermore, xCT has been implicated in the proliferation and multidrug resistance of several types of cancer cells (Chen et al., 2009; Huang et al., 2005; Lo et al., 2008). We carried out this study to determine the function and mechanism of CD44v in controlling redox status in cancer cells through the regulation of xCT-mediated cystine transport.

RESULTS

CD44 Expression Correlates with ROS Defense, and CD44 Ablation Activates ROS-$p38^{MAPK}$ Signaling in Gastrointestinal Cancer Cells

CD44 is a cell surface marker for CSCs in various tumors, and CSCs manifest low intracellular levels of ROS and enhanced protection against ROS-mediated damage (Diehn et al., 2009). Therefore, we hypothesized that CD44 expression is functionally related to ROS defense in cancer cells. To investigate this hypothesis we examined five human gastrointestinal cancer cell lines that differ in CD44 expression status: three gastric cancer lines (MKN28, AGS, KATOIII); and two colorectal cancer lines (HT29, HCT116). These cells were exposed to 0.5 mM hydrogen peroxide (H_2O_2) as an oxidative stressor for 20 min and then examined by fluorescence microscopy after staining with 2′,7′-dichlorofluorescein diacetate (DCFH-DA), a ROS-sensitive fluorescent probe. The hydrolyzed compound DCFH is oxidized to yield dichlorofluorescin (DCF), which is detectable by fluorescence microscopy or flow cytometry (Behl et al., 1994; Suematsu et al., 1992). In contrast to the cell lines (HCT116, HT29, KATOIII) expressing a high level of CD44 ($CD44^{high}$), those negative for CD44 expression ($CD44^{neg}$, MKN28) or expressing CD44 at a low level ($CD44^{low}$, AGS) showed pronounced DCFH-DA staining (Figure 1A). Thus, this result suggested that $CD44^{high}$ gastrointestinal cancer cells have a more efficient ROS defense system than do $CD44^{neg}$ or $CD44^{low}$ cells.

To examine the functional relevance of CD44 expression to ROS defense in $CD44^{high}$ cancer cells, we depleted these cell lines of CD44 by RNA interference (RNAi) (Figure 1B). Flow cytometric analysis revealed that HCT116 cells and HT29 cells depleted of CD44 by transfection with a small interfering RNA (siRNA) specific for CD44 mRNA showed a small increase in DCFH-DA staining compared with those transfected with a control siRNA (Figure 1C; see Figure S1A available online). In KATO III cells, which have a higher basal ROS level than other cell lines, CD44 depletion by transfection with a siRNA specific for CD44 mRNA markedly increased DCFH-DA staining compared with those transfected with a control siRNA (Figure S1A). These results suggest that the increase of ROS levels by CD44 ablation depends on cell context and basal ROS levels.

To exclude the differences of cellular redox status and further examine the role of CD44 on ROS defense ability, we exposed the cells to H_2O_2. CD44-deficient HCT116 cells manifested a markedly greater increase in DCFH-DA staining after exposure to H_2O_2 than did those transfected with the control siRNA (Figure 1C). Similar effects of CD44 ablation on H_2O_2-induced DCF fluorescence were also observed in the other two $CD44^{high}$ cell lines (HT29, KATOIII), although the efficiency of CD44 knockdown differed between the two lines (Figure S1B). These results indicated that CD44 expression contributes to ROS defense in cancer cells.

To investigate further the potential role of CD44 in the cellular response to oxidative stress, we examined the activation of $p38^{MAPK}$, a major target of ROS (Muller, 2009). Depletion of CD44 by RNAi resulted in a marked increase in the phosphorylation (activation) level of $p38^{MAPK}$ in HCT116 cells exposed to H_2O_2 (Figure 1D). The H_2O_2-induced $p38^{MAPK}$ activation and ROS accumulation in CD44-deficient HCT116 cells were completely inhibited by treatment with *N*-acetylcysteine (NAC) (Figures 1D and 1E). Thus, NAC treatment reversed the oxidative stress phenotype of the CD44-depleted cells. These results suggested that CD44 promotes ROS metabolism in cancer cells and thereby suppresses the activation of ROS-$p38^{MAPK}$ signaling.

$CD44^+$ Gastric Tumor Cells Show a Low Level of $p38^{MAPK}$ Phosphorylation In Vivo

To address the functional relevance of CD44 expression to gastric tumorigenesis, we studied a transgenic mouse model of gastric cancer, the *K19-Wnt1/C2mE* or Gan (*g*astric *n*eoplasia) mouse, in which both Wnt and prostaglandin E_2 signaling pathways are activated in the gastric mucosa (Oshima et al., 2006). These transgenic animals develop large, well-differentiated

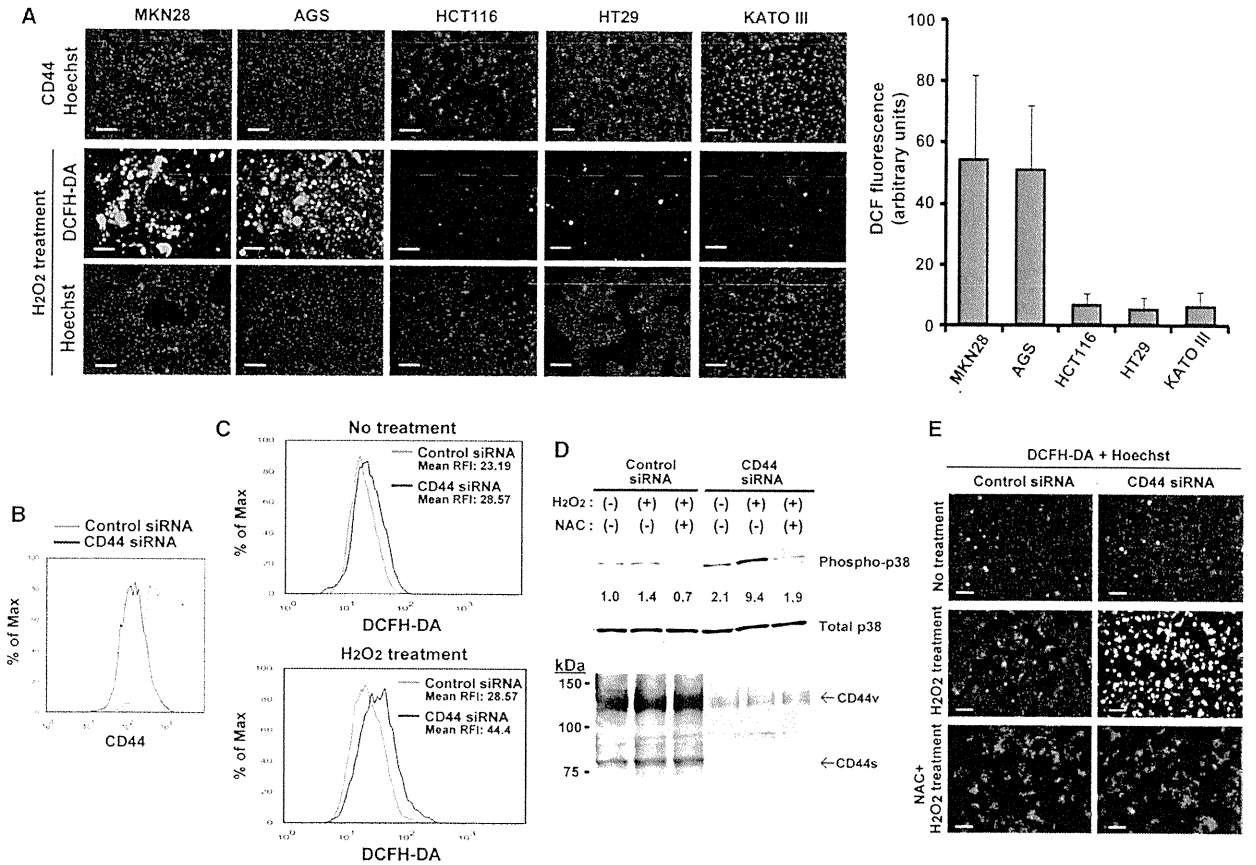

Figure 1. CD44 Contributes to ROS Defense in Gastrointestinal Cancer Cells

(A) Cell lines incubated with 500 μM H_2O_2 for 20 min were stained with DCFH-DA (left, middle panels) and with Hoechst 33342 (left, lower panels) and examined by fluorescence microscopy. Cells not exposed to H_2O_2 were also analyzed with antibodies to CD44 and to Hoechst 33342 staining (left, upper panels). Scale bars, 100 μm. DCF fluorescence intensity (arbitrary units) was determined for >1000 cells in a representative experiment and is presented as mean ± SD values (right panel).

(B) Flow cytometric analysis of CD44 expression on HCT116 cells transfected with control or CD44 siRNAs.

(C) HCT116 cells transfected with control or CD44 siRNAs were treated as in (A) and then stained with DCFH-DA, and subjected to flow cytometric analysis. RFI, relative fluorescence intensity.

(D) HCT116 cells transfected with control or CD44 siRNAs were incubated in the absence or presence of 10 mM NAC for 5 min and then in the additional absence or presence of 500 μM H_2O_2 for 20 min, lysed, and subjected to immunoblot analysis with indicated antibodies. The positions of bands corresponding to variant (CD44v) and standard (CD44s) forms of CD44 are indicated. The fold increase in the intensity of the phospho-$p38^{MAPK}$ band relative to that in the leftmost lane is also shown.

(E) HCT116 cells transfected with control or CD44 siRNAs were treated as in (D) and then stained with DCFH-DA and Hoechst 33342, and examined by fluorescence microscopy. Scale bars, 100 μm.

See also Figure S1.

(intestinal-type) gastric tumors and become moribund around 30–50 weeks of age (Oshima et al., 2006). We first examined the expression of CD44 in the gastric tumors of 30-week-old Gan mice. Reverse transcription (RT) and polymerase chain reaction (PCR) analysis of normal stomach and gastric tumor tissue revealed upregulation of CD44 mRNA in gastric tumors (Figure 2A), indicating that an increase in CD44 gene expression is associated with gastric tumorigenesis. Immunohistochemical analysis also showed that CD44 expression was increased in gastric tumors relative to that in the normal glandular stomach but that its pattern of expression in the tumors was heterogeneous (Figure 2B). We further found that the phosphorylated form of $p38^{MAPK}$, which is normally expressed in the differentiated gastric surface epithelial cells (Figure 2C, lower panel), was preferentially detected in tumor cells that were negative for CD44 staining (Figure 2C, upper panel). We recently showed that CD44 expressed in the tumor cells of Gan mice consists mostly of variant isoforms (CD44v8–10) containing amino acids derived from exons 8–10 (Ishimoto et al., 2010). Furthermore, RT-PCR analysis revealed that CD44v8–10 mRNA, rather than CD44s mRNA, was the dominant form of CD44 mRNA present in the human gastrointestinal cell lines AGS, HCT116, HT29, and KATOIII (Figure S2). Therefore, we next examined the relation between CD44v expression and phosphorylation of

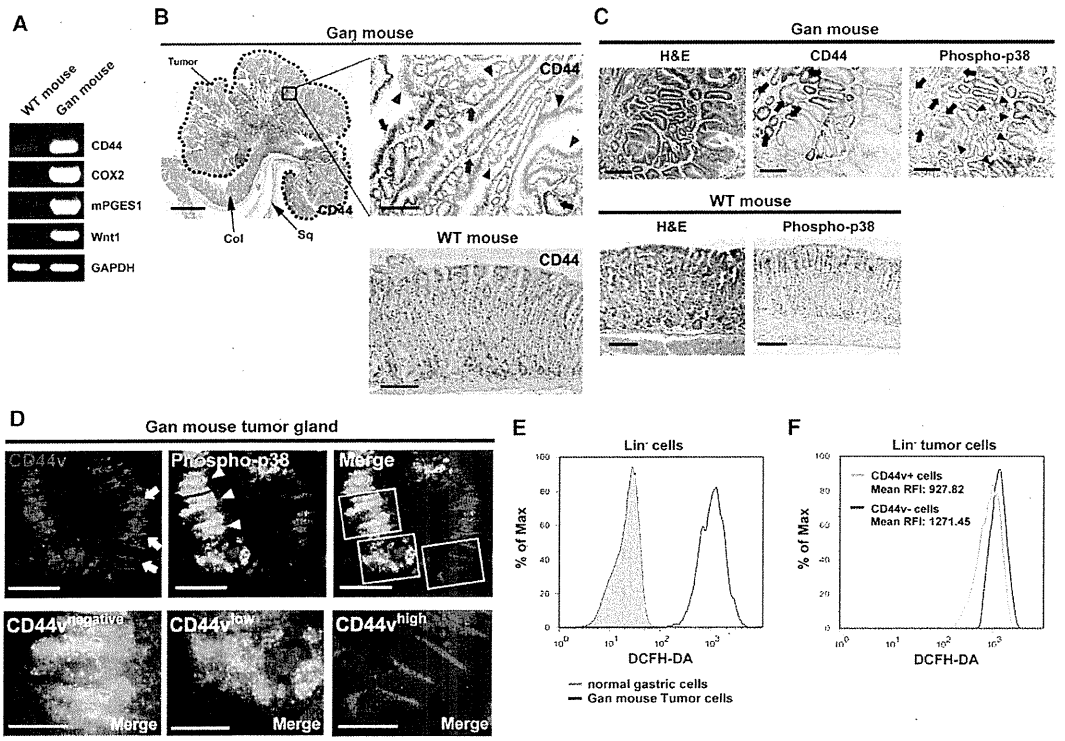

Figure 2. CD44 and Phospho-p38^{MAPK} Expression in Gastric Tumors of Gan Mice

(A) RT-PCR analysis of expression of the CD44 gene and of transgenes in the stomach of wild-type (WT) or Gan mice at 30 weeks of age. Expression of the gene for glyceraldehyde-3-phosphate dehydrogenase (GAPDH) was examined as a control.

(B) CD44 staining in the normal stomach of a WT mouse (lower image) and in a gastric tumor of a 30-week-old Gan mouse (left, upper images). The boxed region in the left image is shown at higher magnification in the right image. Arrows and arrowheads indicate CD44$^+$ and CD44$^-$ tumor cells, respectively. Col, columnar epithelium; Sq, squamous epithelium. Scale bars, 1 mm (left, upper images) and 100 μm (lower image, and right, upper images).

(C) H&E and immunostaining for CD44 and phospho-p38^{MAPK} in a gastric tumor of a 30-week-old Gan mouse (upper images). H&E and immunostaining for phospho-p38^{MAPK} in the normal stomach of a WT mouse (lower images). Arrows and arrowheads indicate inversely correlated expression of CD44 and phospho-p38^{MAPK}, respectively, in tumor cells. Scale bars, 100 μm.

(D) Immunofluorescence staining for CD44v and phospho-p38^{MAPK} together with staining of nuclei with 4′,6-diamidino-2-phenylindole (DAPI). Arrows and arrowheads indicate inversely correlated expression of CD44v and phospho-p38^{MAPK}, respectively, in tumor cells. Scale bars, 20 μm. Lower images show CD44v$^-$, low-, and high-expressing cells at higher magnification of the boxed region in the upper image. Scale bars, 10 μm.

See also Figure S2.

(E) Dissociated tumor cells from Gan mice and glandular stomach cells from WT mice were stained with DCFH-DA and subjected to flow cytometric analysis.

(F) Dissociated tumor cells from Gan mice were subjected to flow cytometric analysis with antibodies to CD44v and DCFH-DA. RFI, relative fluorescence intensity.

p38^{MAPK} with the use of antibodies specific for CD44v. Immunofluorescence analysis revealed that the abundance of phospho-p38^{MAPK} was inversely correlated with CD44v expression within a single tumorous gland (Figure 2D); CD44v$^-$ cells expressed high levels of phospho-p38^{MAPK}, CD44v high-expressing cells did not express phospho-p38^{MAPK}, and CD44v low-expressing cells expressed a moderate level of phospho-p38^{MAPK}. Consistent with our data obtained with the HCT116 cell line (Figure 1D), p38^{MAPK} activation was thus found to be suppressed in CD44v$^+$ cells of mouse gastric tumors compared with that in CD44v$^-$ cells. Our observation that CD44 and phospho-p38^{MAPK} expression appeared to be heterogeneous and inversely correlated within individual tumorous glands of Gan mice suggested that CD44$^+$ tumor cells have an increased capacity for ROS defense. To address this possibility we measured ROS level in tumor cells isolated from Gan mouse by DCFH-DA. Gan mouse tumor cells showed much higher DCFH-DA fluorescence compared with normal mouse gastric cells (Figure 2E), indicating that Gan mouse tumor contains a high level of ROS. We next investigated whether CD44v$^+$ tumor cells contain a lower level of ROS compared with CD44v− cells. DCFH-DA staining revealed that CD44v$^+$ tumor cells contain a much lower level of ROS than CD44v− cells (Figure 2F), suggesting that CD44 expression status is associated with ROS defense ability of tumor cells.

Upregulation of Antioxidant Gene Expression in CD44$^+$ Tumor Cells

We next examined the expression of antioxidant genes in tumor cells isolated from Gan mice by fluorescence-activated cell sorting (FACS). Thus, lineage marker (Lin)-negative cells that were CD44$^+$ or CD44$^-$ were isolated from the gastric tumors of 30-week-old Gan mice (Figure 3A) and subjected to cDNA

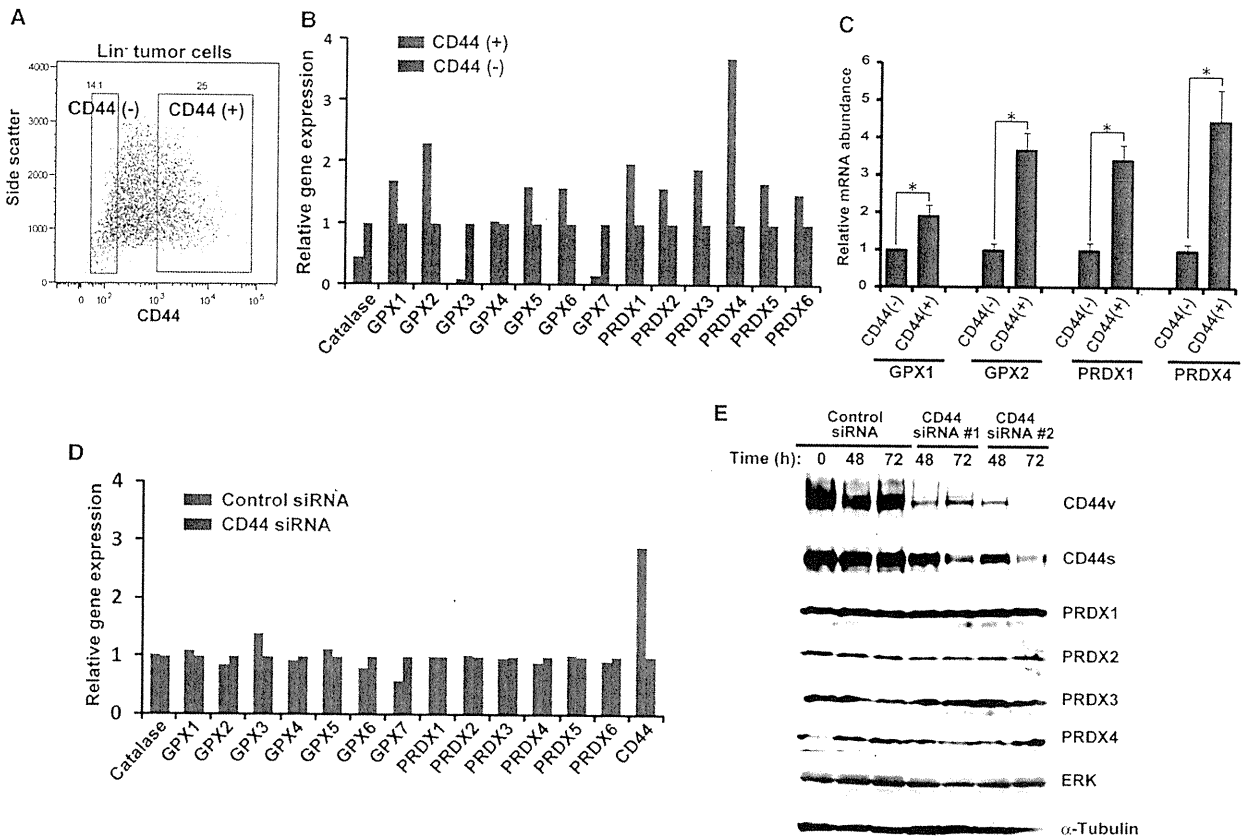

Figure 3. Upregulation of Antioxidant Gene Expression in CD44$^+$ Gastric Tumor Cells Isolated from Gan Mice

(A) Dissociated tumor cells from Gan mice were subjected to flow cytometric analysis with antibodies to CD44. See also Figures S3A and S3B.

(B) Expression of the indicated antioxidant enzyme genes in CD44$^+$ cells relative to that in CD44$^-$ cells isolated as in (A), as determined by cDNA microarray analysis. Data are from a representative experiment.

(C) Antioxidant enzyme gene expression in CD44$^+$ cells relative to that in CD44$^-$ cells isolated as in (A), as determined by quantitative RT-PCR analysis. Data were normalized by the amount of GAPDH mRNA and are mean ± SD from three independent experiments. *$p < 0.01$.

(D) Antioxidant enzyme gene expression in HCT116 cells transfected with a control siRNA relative to that in cells transfected with a CD44 siRNA, as determined by cDNA microarray analysis. Data are from a representative experiment. See also Figure S3C.

(E) Immunoblot analysis of CD44 and PRDX isoforms in HCT116 cells transfected with a control siRNA or CD44 siRNAs (#1 or #2) for the indicated times. ERK and α-tubulin were similarly analyzed as loading controls.

microarray analysis. Compared with CD44$^-$ cells, CD44$^+$ cells manifested increased expression of Wnt target genes but only low levels of expression of marker genes for gastric differentiation, including those for MUC5AC, gastric H^+/K^+-ATPase subunit beta (Atp4b), gastric intrinsic factor (Gif), and pepsinogen C (Pgc) (Figures S3A and S3B), suggesting that CD44$^+$ tumor cells are maintained in an undifferentiated state. The expression of several key antioxidant genes, including those for glutathione peroxidase (GPX) and peroxiredoxin (PRDX) isoforms, was found to be increased in CD44$^+$ tumor cells compared with that in CD44$^-$ cells (Figure 3B), consistent with the notion that CD44$^+$ tumor cells have an increased capacity for ROS defense. Quantitative RT-PCR analysis confirmed that the abundance of mRNAs for GPX1 and GPX2, which are major H_2O_2-reducing antioxidant enzymes in the gastrointestinal tract, as well as that of mRNAs for PRDX1 and PRDX4 was significantly higher in CD44$^+$ tumor cells than in CD44$^-$ cells (Figure 3C). Similar to our observations for CD44$^+$ gastric tumor cells, breast CSCs have previously been found to express antioxidant enzyme genes at increased levels and to show an enhanced ROS defense ability compared with their nontumorigenic progeny (Diehn et al., 2009).

We next examined whether depletion of CD44 might affect antioxidant gene expression in cancer cells. Thus, HCT116 cells were transfected with CD44 or control siRNAs and subjected to cDNA microarray analysis or RT and real-time PCR analysis. Although the CD44 siRNA was found to deplete the cells of CD44 mRNA, the expression of antioxidant genes was largely unaffected (Figures 3D; Figure S3C). We also examined the abundance of PRDX isoforms in CD44-depleted HCT116 cells by immunoblot analysis and found that CD44 depletion did not affect the amounts of PRDX1, -2, -3, and -4 (Figure 3E). Therefore, these results suggested that, although several antioxidant enzyme genes are highly expressed in CD44$^+$ cancer cells

in vivo, the CD44-mediated antioxidative effect in cultured cancer cells is largely independent of regulation of antioxidant gene expression.

CD44v Regulates the Intracellular Level of GSH

On the basis of our observation that CD44 depletion did not affect antioxidant gene or protein expression in cancer cells (Figures 3D and 3E), we examined whether it might alter the intracellular level of GSH in $CD44^{high}$ cancer cells. Depletion of CD44 was achieved with two different siRNAs that target different sequences of CD44 mRNA (Figure S4A) and resulted in a pronounced reduction in the intracellular GSH content of HCT116 cells (Figure 4A), suggesting that CD44 contributes to the regulation of the intracellular level of GSH. To examine whether forced expression of CD44 affects intracellular GSH content, we transiently transfected 293T cells (a transformed human kidney cell line with a high transfection efficiency) with an expression vector either for CD44s or for CD44v8–10, a major variant isoform of CD44 in human gastrointestinal malignancies (Figure S2) (Tanabe et al., 1993). The amount of GSH in cells expressing CD44v was found to be significantly greater than that in those expressing CD44s or in those transfected with the empty vector (Figure 4B), suggesting that CD44v regulates intracellular GSH content. Importantly, the increase of GSH content achieved by CD44v8–10 expression was comparable to that achieved by treatment with NAC, which is a precursor of GSH and functions as an antioxidant (Figure 4B). All these findings suggest that CD44v8–10 expression promotes GSH synthesis. To further confirm this hypothesis, we stably transfected MKN28 cells ($CD44^{neg}$) with an expression vector either for CD44s or for CD44v. The resulting CD44s- or CD44v-expressing MKN28 cells (Figure S4B) were incubated for 24 hr with L-buthionine-sulfoximine (BSO), which inhibits γ-glutamylcysteinyl synthase and thereby depletes intracellular GSH, and were then allowed to recover for 24 hr in BSO-free medium. The CD44v-expressing MKN28 cells, but not the CD44s-expressing cells, were found to contain a significantly greater amount of GSH at this time compared with cells transfected with the empty vector (Figure 4C). Thus, this result suggested that CD44v, but not CD44s, promotes GSH synthesis. Given that increased GSH synthesis promotes resistance to anticancer agents that induce ROS-mediated cytotoxicity (Trachootham et al., 2009), we next investigated whether CD44v-dependent GSH synthesis promotes the viability of cells exposed to H_2O_2 or to ROS-inducing anticancer drugs such as cisplatin (CDDP) and docetaxel (DTX). We found that CD44v-expressing MKN28 cells were more resistant to H_2O_2, CDDP, and DTX than were cells stably transfected with the empty vector (Figure 4D). These results suggested that promotion of GSH synthesis by CD44v results in enhancement of cellular antioxidative capacity and thereby promotes resistance to common chemotherapeutic drugs.

Given that the availability of cysteine is rate limiting for GSH synthesis (Ishii et al., 1987), we next investigated the effect of CD44 depletion by RNAi on the amino acid content of HCT116 cells. This analysis revealed that CD44 depletion resulted in an ~67% decrease in the amount of cysteine, whereas the amounts of other amino acids including glutamate and glycine were not similarly affected (Figure 4E). Given that the intracellular level of cysteine is determined largely by the function of the xc^- system, which exchanges extracellular cystine for intracellular glutamate, with the cystine then being rapidly converted to cysteine and utilized for GSH synthesis (Lo et al., 2008), we hypothesized that CD44 might influence the function of this transporter. To test this hypothesis we directly measured cystine uptake in HCT116 cells by incubating the cells with ^{15}N-labeled L-cystine and then determining the intracellular contents of the mass-labeled cysteine by CE-MS-based metabolome analysis (Shintani et al., 2009). We found that CD44 ablation by RNAi resulted in significant inhibition of cystine uptake in HCT116 cells (Figure 4F; Table S1), suggesting that CD44 affects the function of the cystine transporter.

CD44 Depletion Reduces the Cell Surface Expression and Stability of xCT

The xCT subunit confers substrate specificity on the xc^- system, allowing the cellular uptake of cystine in exchange for intracellular glutamate, and is essential for cellular protection from oxidative stress (Huang et al., 2005; Sato et al., 2005). To examine whether the expression of xCT at the cell surface is related to CD44 expression in cancer cells, we prepared a monoclonal antibody that recognizes the extracellular domain of human xCT and then measured the amount of xCT at the surface of the $CD44^{high}$ cancer cell lines HCT116, HT29, and KATOIII by flow cytometry. The expression level of xCT at the surface of these $CD44^{high}$ cancer cells was substantially higher than that apparent for $CD44^{neg}$ (MKN28) cells (Figure 5A), suggesting that cell surface expression of xCT might be related to CD44 expression. On the other hand we found that the amount of xCT mRNA in these various cell lines was not correlated with xCT protein expression at the cell surface (Figure S5A). We also examined the possible effect of CD44 on the abundance of xCT mRNA in HCT116 cells by RNAi. CD44 ablation resulted in an increase in the amount of xCT mRNA, and this effect was inhibited by NAC treatment (Figures S5B and S5C), indicating that the increase in xCT mRNA abundance induced by CD44 depletion is due to increased intracellular accumulation of ROS. The abundance of xCT mRNA was previously shown not to correlate with the intracellular level of GSH in NCI-60 cancer cells (Huang et al., 2005) but was found to be increased as a result of cystine deprivation (Sasaki et al., 2002). Thus, our results suggested that the amount of xCT mRNA is regulated by the intracellular ROS level, whereas cell surface expression of xCT might be regulated by CD44 expression status.

To examine the relevance of CD44 to the subcellular localization of xCT, we performed immunocytofluorescence analysis by confocal microscopy. Most xCT immunofluorescence at the surface of HCT116 cells was found to colocalize with CD44 immunofluorescence, whereas RNAi-mediated CD44 ablation reduced the amount of xCT at the plasma membrane (Figure 5B). Flow cytometry also revealed that CD44 ablation reduced the amount of xCT at the cell surface without affecting the cell surface expression of CD98hc in HCT116 cells (Figure 5C), suggesting that CD44 regulates the subcellular localization of xCT, but not that of CD98hc. We next investigated whether CD44 expression might affect the stability of xCT by establishing HCT116 cells that stably express either a short hairpin RNA (shRNA) specific for CD44 mRNA or a corresponding scrambled

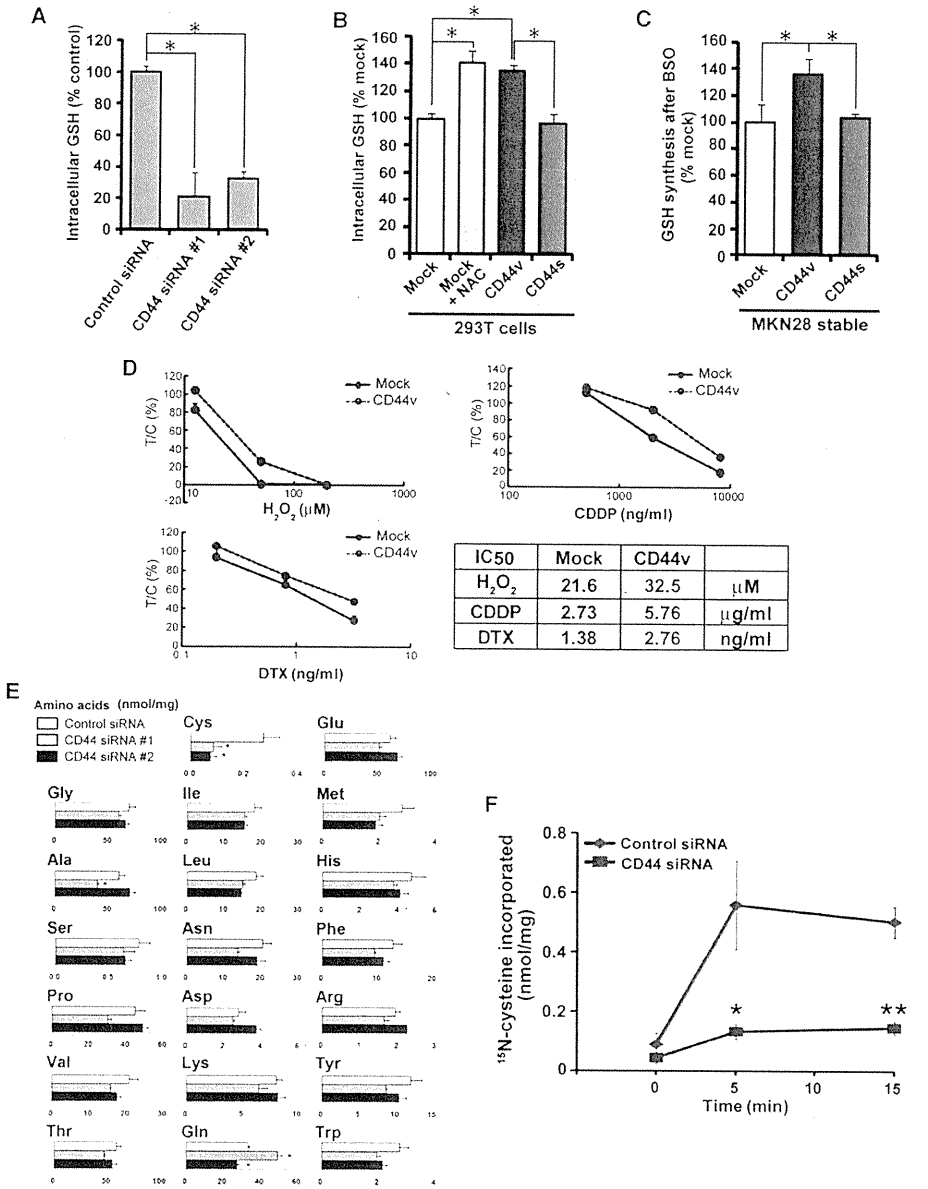

Figure 4. CD44 Expression Correlates with the Intracellular Level of GSH

(A) GSH content of HCT116 cells transfected with CD44 siRNAs relative to that of those transfected with a control siRNA. Data are mean ± SD from three independent experiments. *$p < 0.01$. See also Figure S4A.

(B) GSH content of HEK293T cells incubated with 1 mM NAC for 12 hr, expressing CD44v or CD44s relative to that of those transfected with the empty vector (mock). Data are mean ± SD from three independent experiments. *$p < 0.01$.

(C) MKN28 cells stably expressing CD44v or CD44s, or those stably transfected with the empty vector (mock), were incubated with 500 μM BSO for 24 hr and then allowed to recover in BSO-free medium for 24 hr. GSH content was analyzed as in (C). Data are mean ± SD from three independent experiments. *$p < 0.01$. See also Figure S4B.

(D) MKN28 cells stably expressing CD44v, or those stably transfected with the empty vector (mock), were incubated for 72 hr with the indicated concentrations of H_2O_2, CDDP, or DTX and then assayed for cell viability; data are expressed as treated/control cell ratio and are mean ± SD from three independent experiments. The median inhibitory concentration (IC_{50}) values are also shown.

(E) Amino acid contents of HCT116 cells transfected with the control siRNA or with CD44 siRNAs (#1 or #2). Data are expressed as mean ± SE from three separate experiments. *$p < 0.03$ versus the value for cells transfected with the control siRNA. (F) Differences in $^{15}N_2$-cystine uptake between HCT116 cells transfected with CD44 siRNA and those transfected with the control siRNAs. Data are expressed as mean ± SE from five separate experiments. *$p < 0.05$. **$p < 0.01$ versus the values for the cells transfected with the control siRNA.

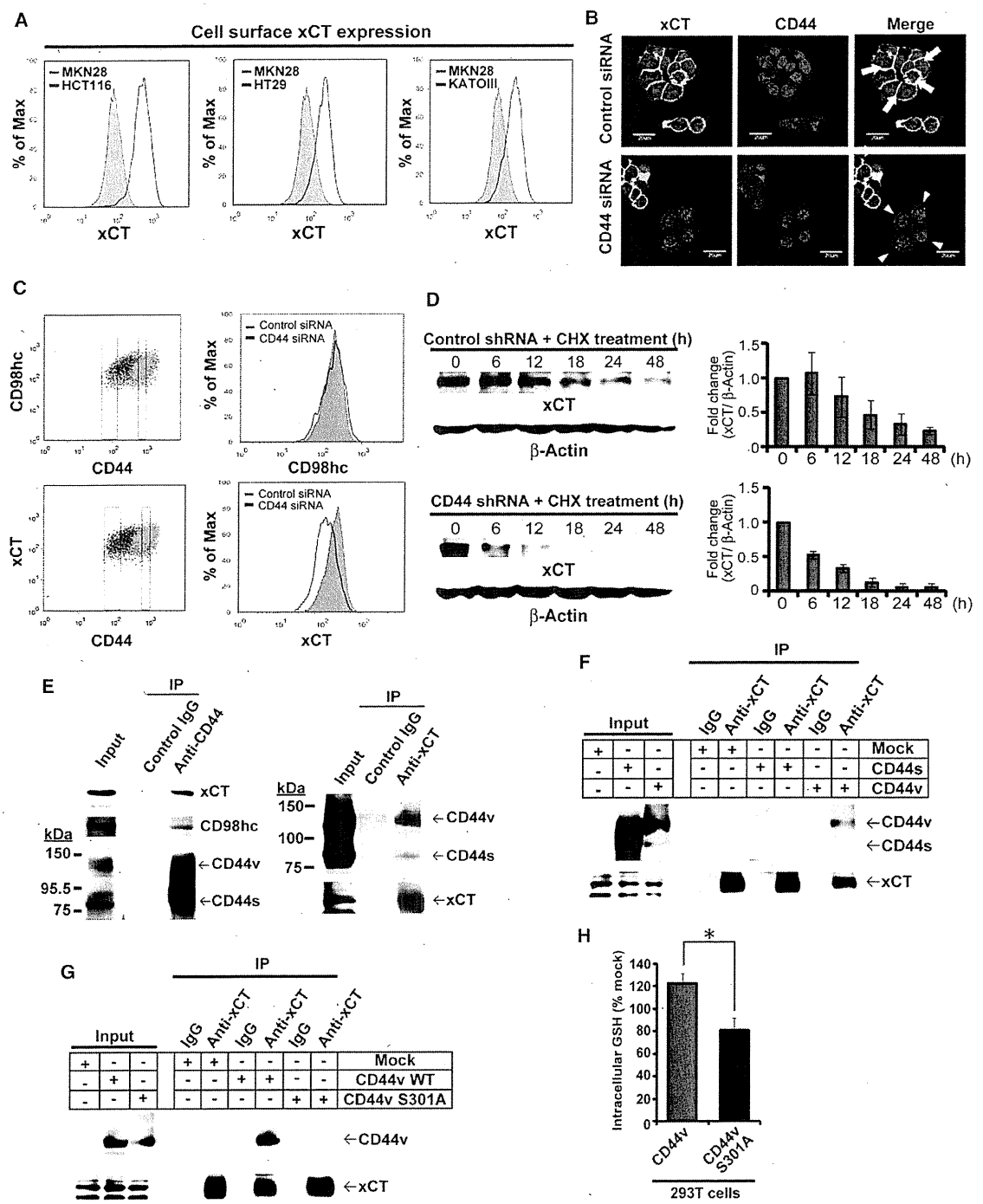

Figure 5. CD44 Regulates Cell Surface Expression of xCT, but Not that of CD98hc

(A) Flow cytometric analysis of cell surface xCT expression in HCT116, HT29, and KATOIII cells relative to that on MKN28 cells. Cells were stained with rat monoclonal antibodies to human xCT, which recognize the extracellular domain of xCT.

(B) Immunofluorescence analysis of xCT and CD44 in HCT116 cells transfected with control or CD44 siRNAs. Nuclei were also stained with DAPI. Arrows indicate colocalization of xCT and CD44 at the cell surface; arrowheads indicate loss of surface expression of xCT in cells depleted of CD44. Scale bars, 20 μm.

(C) Flow cytometric analysis of CD98hc, xCT, and CD44 expression at the surface of HCT116 cells transfected with control or CD44 siRNAs. Cells were stained with antibodies to CD44 as well as with antibodies to CD98hc or to xCT.

(control) shRNA (Figure S5D). We measured the protein levels of xCT by both immunoblot and FACS analyses. Treatment of the cells with the protein synthesis inhibitor cycloheximide (CHX) revealed that the levels of xCT in the cells expressing the CD44 shRNA were reduced significantly faster than those in the cells expressing the control shRNA (Figures 5D; Figure S5E), suggesting that CD44 expression enhances the stability of xCT protein.

CD44v Interacts with and Stabilizes xCT at the Plasma Membrane

Therefore, we hypothesized that CD44 and xCT interact at the plasma membrane and that this molecular interaction stabilizes the membrane localization of xCT and thereby promotes cystine uptake in $CD44^{high}$ cancer cells. To test this hypothesis we examined whether CD44 and xCT interact with each other by immunoprecipitation analysis. Such analysis with antibodies to CD44 revealed that both xCT and CD98hc indeed physically interact with CD44 (Figure 5E). Furthermore, such analysis with antibodies to xCT showed that xCT interacts preferentially with 130 kDa CD44v rather than with the 85 kDa CD44s isoform (Figure 5E). We recently found that CD44v (v6–10, v7–10, and v8–10) was the predominant form of CD44 expressed in the gastric tumors of Gan mice (Ishimoto et al., 2010). Thus, these observations suggested that CD44v may play a key role in resistance to oxidative stress in gastrointestinal cancer cells and thereby might promote tumor development.

To confirm that xCT preferentially interacts with CD44v, we expressed recombinant CD44s or CD44v in 293T cells, which contain only low levels of endogenous CD44, and performed immunoprecipitation analysis with antibodies to xCT. Such analysis revealed that xCT specifically interacted with CD44v, not with CD44s (Figure 5F). Together with our observation that forced expression of CD44v, but not that of CD44s, increased the intracellular GSH content in 293T cells (Figure 4B), these results suggested that CD44v interacts with and stabilizes xCT and thereby increases intracellular GSH content.

To further determine whether variant region of CD44v is indeed required for the interaction of CD44v and xCT, we generated an expression plasmid encoding the S301A mutant of CD44v (Figure S5F). Given that the v8–10 region of CD44v contains consensus motifs for an N-linked glycosylation site (Asn-X-Ser/Thr) (Dougherty et al., 1991), the CD44v S301A is considered to be an N-linked glycosylation site mutant. The immunoprecipitation analysis revealed that the CD44v S301A failed to interact with xCT (Figure 5G), suggesting that the v8–10 region of CD44 is required for the specific interaction between CD44v and xCT. Furthermore, forced expression of the CD44v S301A failed to increase basal GSH level in 293T cells (Figure 5H). These results suggest that specific interaction of CD44v and xCT maintains a high level of GSH in cancer cells.

To determine whether xCT contributes to the ROS defense mechanism of $CD44^{high}$ (HCT116) cancer cells, we investigated the effect of xCT depletion by RNAi (Figure S5G) on ROS-scavenging ability. Ablation of xCT resulted in a significant increase in DCFH-DA staining in cells exposed to H_2O_2 (Figure S5H), as did treatment with BSO (Figure S5I), suggesting that xCT-mediated cystine uptake and consequent GSH synthesis are important for the ROS-scavenging ability of cancer cells. Furthermore, we found that H_2O_2-induced activation of $p38^{MAPK}$ was enhanced by xCT depletion (Figure S5J), as it was by CD44 ablation (Figure 1D). Thus, these results suggested that both CD44 and xCT are required for suppression of ROS-induced $p38^{MAPK}$ activation.

CD44 Ablation Reduces the Number of Proliferating Tumor Progenitor Cells and Inhibits Gastric Tumor Development in Gan Mice

To examine whether CD44 expression affects tumor cell expansion during gastric tumorigenesis in vivo, we crossed Gan mice with CD44 knockout ($CD44^{-/-}$) mice, which show no overt phenotype during development (Schmits et al., 1997), in order to generate $CD44^{-/-}$ Gan animals. Tumors were markedly smaller in $CD44^{-/-}$ Gan mice than in Gan mice at 30 weeks of age and thereafter, whereas tumor size was similar in animals of the two genotypes up to 20 weeks of age (Figures 6A and 6B), suggesting that CD44 is required for the maintenance of tumor cell proliferation. Furthermore, hematoxylin and eosin staining (H&E) revealed that $CD44^{-/-}$ Gan mice only gave rise to hyperplastic tumors (Figure 6B), suggesting that CD44 expression affects gastric tumor grade in Gan mice.

We next investigated the mechanism underlying the difference in tumor size between Gan mice and $CD44^{-/-}$ Gan mice. The proportion of proliferating tumor cells that incorporated bromodeoxyuridine (BrdU) was significantly smaller in $CD44^{-/-}$ Gan mice than in Gan mice (Figure 6C), indicating that the number of proliferating progenitor cells was reduced in the CD44-deficient hyperplastic tumors. In contrast the proportion of apoptotic cells in tumors did not differ between mice of the two genotypes (Figure 6D). Thus, these results indicated that CD44 contributes to the proliferation of gastric tumor cells rather than to cell survival in Gan mice.

(D) Left panels show immunoblot analysis of xCT and β-actin (loading control) in HCT116 cells stably expressing control or CD44 shRNAs and exposed to CHX (40 μg/ml) for the indicated times. In the right panels, mean values ±SD from three independent experiments for the xCT/β-actin band intensity ratio relative to the corresponding value for time zero (0) are shown. See also Figure S5E.

(E) HCT116 cell lysates were subjected to immunoprecipitation (IP) with antibodies to CD44 (IM7) or to xCT, or with control immunoglobulin G (IgG), and the resulting precipitates, as well as the original cell lysates (input), were subjected to immunoblot analysis with antibodies to xCT, to CD98hc, or to CD44 (anti-CD44cyto).

(F) Lysates of HEK293T cells expressing CD44v or CD44s, or of those transfected with the empty vector (mock), were subjected to immunoprecipitation with antibodies to xCT or with control IgG, and the resulting precipitates, as well as the original cell lysates (input), were subjected to immunoblot analysis with antibodies to xCT or to CD44 (anti-CD44cyto).

(G) Lysates of HEK293T cells expressing CD44v or CD44v (S301A), or those transfected with the empty vector (mock), were subjected to IP with antibodies to xCT or with control IgG, and the resulting precipitates, as well as the original cell lysates (input), were subjected to immunoblot analysis with antibodies to xCT or to CD44 (anti-CD44cyto).

(H) HEK293T cells expressing CD44v or CD44v (S301A), or those transfected with the empty vector (mock), were analyzed for intracellular GSH content. Data are expressed relative to the value for mock-transfected cells and are mean ± SD from three independent experiments. *$p < 0.01$. See also Figure S5F.

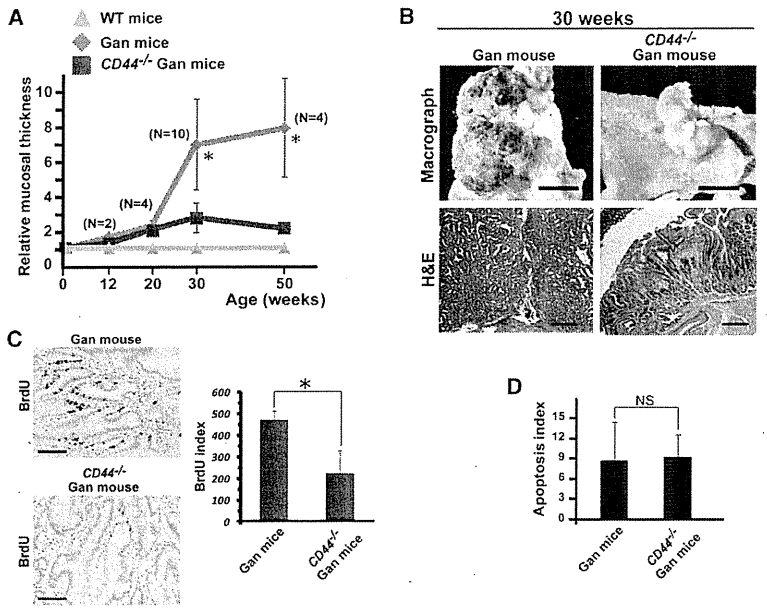

Figure 6. Growth of Gastric Tumors in Gan Mice Is Suppressed by CD44 Ablation

(A) Gastric mucosal thickness in Gan or *CD44*$^{-/-}$ Gan mice at the indicated ages relative to that in age-matched wild-type (WT) mice. Data are mean ± SD for the indicated number of animals. *$p < 0.05$ versus the corresponding value for *CD44*$^{-/-}$ Gan mice.

(B) Macroscopic images and H&E of gastric tumors of Gan and *CD44*$^{-/-}$ Gan mice at 30 weeks of age. Scale bars, 5 mm (upper panels) and 100 μm (lower panels).

(C) BrdU incorporation in gastric tumors of 30-week-old Gan or *CD44*$^{-/-}$ Gan mice (left panels). Scale bars, 100 μm. The BrdU-labeling index was determined as mean ± SD values for five mice of each genotype (right panel); *$p < 0.02$.

(D) Apoptosis index for gastric tumors of 30-week-old Gan or *CD44*$^{-/-}$ Gan mice. Data are mean ± SD for four mice of each genotype. NS, not significant.

CD44 Ablation Induces p38^{MAPK} Activation and p21$^{CIP1/WAF1}$ Upregulation in Gastric Tumors of Gan Mice

Given that sustained activation of p38^{MAPK} is a characteristic of cells with a high ROS level in vivo (Dolado et al., 2007), we examined whether ablation of CD44 increases the abundance of phospho-p38^{MAPK} in gastric tumor cells. The region containing cells positive for phospho-p38^{MAPK} was markedly extended in hyperplastic tissue of *CD44*$^{-/-}$ Gan mice compared with that in tumors of Gan mice (Figure 7A). Furthermore, immunoblot analysis revealed that the amount of phospho-p38^{MAPK} was greater in CD44-deficient hyperplastic tumors than in CD44^{+} tumors (Figures 7B and 7C) and that CD44v, rather than CD44s, was preferentially expressed in the latter tumors (Figure 7B). We next investigated the relation between CD44v expression and p38^{MAPK} signaling in human gastric cancer. The staining patterns of CD44v and phospho-p38^{MAPK} were inversely correlated in tumorous glands of human gastric adenocarcinoma (Figure S6). Together, these results suggested that CD44v negatively regulates p38^{MAPK} activity and that ablation of CD44v induces tumor cells to adopt a more differentiated and less proliferative state through activation of p38^{MAPK}.

We next investigated whether the extension of the tumor region positive for p38^{MAPK} phosphorylation apparent in *CD44*$^{-/-}$ Gan mice might be due to the loss of the influence of CD44 on the plasma membrane localization of xCT. Immunohistochemical analysis revealed that genetic ablation of CD44 resulted in a marked reduction in the amount of xCT at the cell surface (Figure 7D), suggesting that the CD44-xCT axis might regulate p38^{MAPK} signaling through modulation of the intracellular ROS level in gastric tumor cells.

To explore further the molecular mechanism underlying p38^{MAPK}-mediated tumor growth suppression, we examined the expression of p21$^{CIP1/WAF1}$, which is a major downstream component of the pathway by which p38^{MAPK} inhibits cell proliferation (Han and Sun, 2007) and participates in the differentiation of gastric epithelial cells (Katz et al., 2005). Quantitative RT-PCR analysis revealed that CD44 ablation resulted in a significant increase both in the amount of p21$^{CIP1/WAF1}$ mRNA (Figure 7E) and in that of the mRNA for the gastric differentiation marker MUC5AC (Figure 7F) in gastric tumors of Gan mice. Together, these results suggested that CD44 ablation triggers growth arrest in immature and proliferative tumor cells through activation of p38^{MAPK} and upregulation of p21$^{CIP1/WAF1}$, resulting in the suppression of tumor progression through the induction of cell differentiation, in the Gan mouse model.

The xCT Inhibitor Sulfasalazine Suppresses CD44-Dependent Tumor Growth and Promotes Activation of p38^{MAPK} in Tumor Cells In Vivo

We next examined whether xCT contributes to CD44-dependent tumor growth. HCT116 cells stably expressing CD44 shRNA formed significantly smaller tumors in nude mice than did those expressing a control shRNA (Figure 8A), suggesting that HCT116 cells form tumors in vivo in a CD44-dependent manner. Furthermore, immunoblot analysis revealed that RNAi-mediated CD44 knockdown markedly increased the phosphorylation of p38^{MAPK} in the tumor cells (Figure 8B), indicating that CD44-dependent tumor growth is associated with the suppression of p38^{MAPK}-mediated signaling. Sulfasalazine is a well-characterized specific inhibitor of xCT-mediated cystine transport and has been shown to inhibit the growth, invasion, and metastasis of several types of cancer (Chen et al., 2009; Gout et al., 2001; Lo et al., 2008). We found that intraperitoneal administration of sulfasalazine inhibited the growth of tumors formed by HCT116 cells in nude mice (Figure 8C), suggesting that the function of xCT plays a role in the expansion of CD44^{+} tumor cells in vivo. Furthermore, immunohistochemical analysis revealed that sulfasalazine treatment stimulated the phosphorylation of p38^{MAPK} in HCT116 tumor cells in vivo compared with that apparent in mice treated with saline (Figure 8D). Immunoblot analysis of tumor lysates also showed that sulfasalazine treatment increased p38^{MAPK} activation (Figure 8D), as did RNAi-mediated CD44

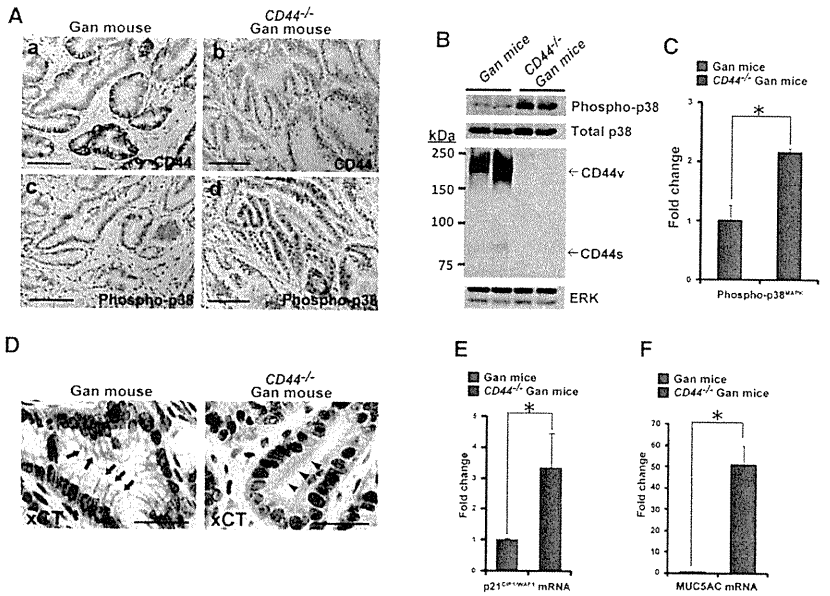

Figure 7. CD44 Ablation in Gastric Tumors Increases the Abundance of Phospho-p38^{MAPK} and Upregulates p21$^{CIP1/WAF1}$

(A) Immunostaining of CD44 (a and b) and phospho-p38^{MAPK} (c and d) in gastric tumors of 30-week-old Gan (a and c) or *CD44*$^{-/-}$ Gan (b and d) mice. Scale bars, 100 μm. See also Figure S6.

(B) Immunoblot analysis of phospho-p38^{MAPK}, total p38^{MAPK}, CD44, and ERK (loading control) in lysates of gastric tumors from 30-week-old Gan or *CD44*$^{-/-}$ Gan mice.

(C) Amount of phospho-p38^{MAPK} in gastric tumors of 30-week-old *CD44*$^{-/-}$ Gan mice relative to that in those of Gan mice, as determined by immunoblot analysis. Data are mean ± SD for three mice of each genotype. *$p < 0.01$.

(D) Immunostaining of xCT in gastric tumors of 30-week-old Gan or *CD44*$^{-/-}$ Gan mice. Arrows indicate expression of xCT at the plasma membrane in tumors of Gan mice, whereas arrowheads indicate the loss of xCT expression at the plasma membrane in tumors of *CD44*$^{-/-}$ Gan mice. Scale bars, 50 μm.

(E) Quantitative RT-PCR analysis of p21$^{CIP1/WAF1}$ mRNA in tumors of 30-week-old *CD44*$^{-/-}$ Gan mice relative to that in those of Gan mice. Data were normalized by the amount of GAPDH mRNA and are mean ± SD for three mice of each genotype. *$p < 0.02$.

(F) Quantitative RT-PCR analysis of MUC5AC mRNA in tumors of 30-week-old *CD44*$^{-/-}$ Gan mice relative to that in those of Gan mice. Data were normalized by the amount of GAPDH mRNA and are mean ± SD for three mice of each genotype. *$p < 0.01$.

knockdown (Figure 8B). Thus, these results suggested that the activity of xCT plays a role in the ability of CD44$^+$ tumor cells to evade oxidative stress and p38^{MAPK}-mediated growth suppression in vivo.

Finally, we examined whether suppression of xCT function by sulfasalazine might enhance the effect of the anticancer drug CDDP on tumor growth. The antitumor effect of CDDP at a low dose (2 mg/kg) was significantly enhanced by treatment with sulfasalazine (Figure 8E), suggesting that sulfasalazine reduces the ROS defense capacity of cancer cells and sensitizes them to available chemotherapeutic drugs.

DISCUSSION

Our results revealed a function of CD44v that contributes to the ROS resistance of gastrointestinal cancer cells. CD44$^+$ gastric tumor cells of Gan mice were shown to express antioxidant genes at higher levels compared with CD44$^-$ tumor cells. We found that CD44$^+$ tumor cells expressed Wnt target genes significantly higher than CD44$^-$ tumor cells (Figure S3A). Given that Wnt signals have been shown to be activated in stem-like cancer cells (Vermeulen et al., 2010), we assume that CD44$^+$ fraction contains more stem-like cells than CD44$^-$ fraction. The previous report demonstrated that the CD44$^+$ breast CSCs manifest upregulation of antioxidant genes (Diehn et al., 2009). Therefore, we speculate that the differences in expression of antioxidant genes in CD44$^+$ and CD44$^-$ fractions are due to the proportion of stem-like tumor cells included in each fraction. However, in the present study we also show that CD44 ablation suppressed the synthesis of the nonenzymatic antioxidant GSH without affecting the level of antioxidant gene expression in cultured cancer cells, indicating that CD44-mediated ROS resistance is largely independent of such antioxidant gene expression. Furthermore, we found that CD44v interacts with and stabilizes the cystine transporter subunit xCT and thereby regulates the intracellular level of GSH in CD44$^+$ cancer cells, resulting in suppression of p38^{MAPK}- and p21$^{CIP1/WAF1}$-mediated growth inhibition. These results indicate that ROS defense in CD44$^+$ cancer stem-like cells is supported by CD44v enhancement of GSH synthesis in addition to high levels of antioxidant gene expression. We are not able to rule out the possibility that CD44 directly or indirectly controls the expression of antioxidant genes in CD44$^+$ cancer stem-like cells in vivo, thus with this issue requiring further investigation.

Recent studies have indicated that increased levels of ROS promote aging of hematopoietic stem cells (Ito et al., 2006) and that, in *Drosophila*, high ROS levels sensitize hematopoietic progenitors to the induction of differentiation (Owusu-Ansah and Banerjee, 2009). On the other hand, CSCs as well as normal stem cells possess an enhanced ROS defense system (Diehn et al., 2009; Phillips et al., 2006). Our results now show that CD44 expression correlates with ROS resistance in cancer cells as a result of the enhancement of GSH synthesis by CD44. Thus, expression of CD44 might serve as a functional marker for CSCs with immature and ROS-resistant properties in various tumor types.

CD44 is synthesized in multiple isoforms as a result of alternative mRNA splicing (Ponta et al., 2003). We and others have previously shown that the expression of CD44v, but not that of CD44s, is associated with progression of human gastrointestinal malignancies (Tanabe et al., 1993). Furthermore, we have recently shown that quiescent or slow-cycling gastric stem or progenitor cells that reside in the normal mouse stomach and undergo expansion during tumorigenesis express a high level

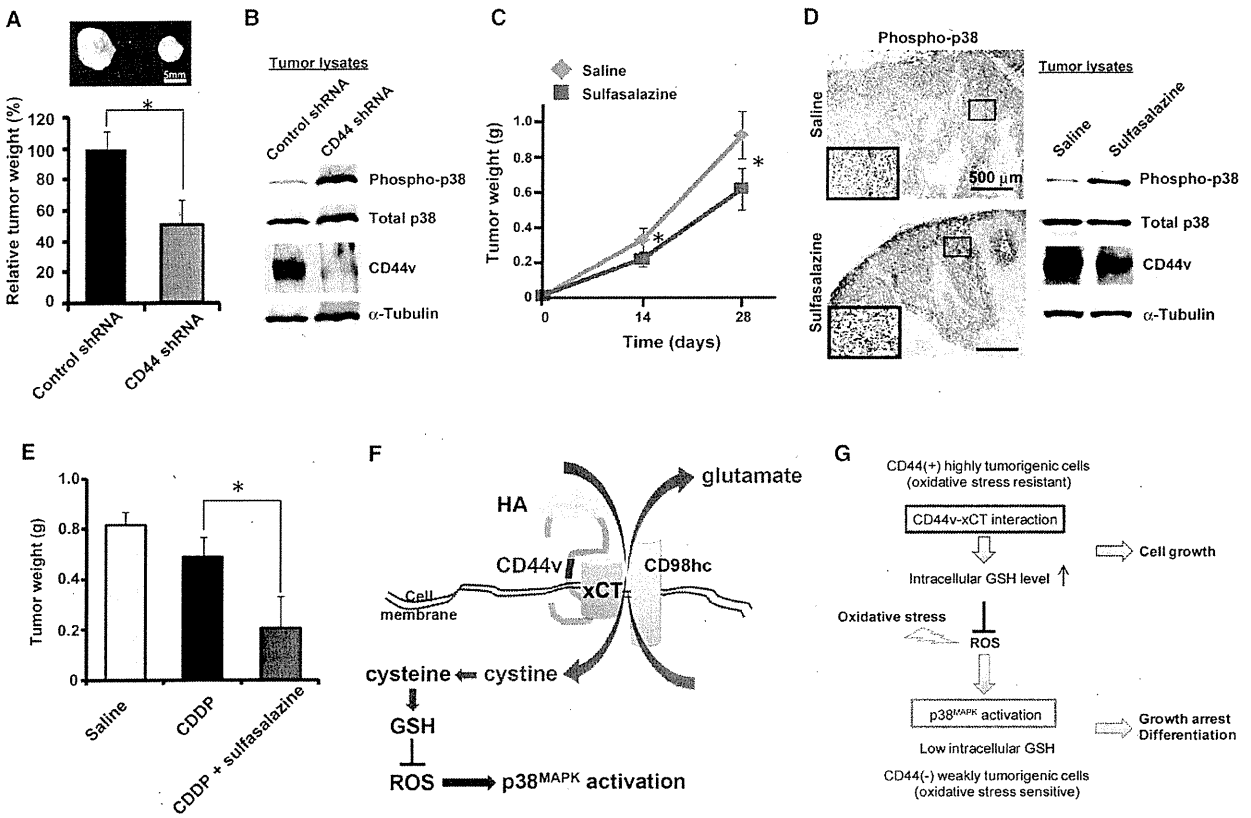

Figure 8. Inhibition of xCT Function Increases $p38^{MAPK}$ Activity in Tumor Cells and Suppresses CD44-Dependent Tumor Growth In Vivo

(A) Macroscopic images of tumors formed in nude mice by HCT116 cells stably expressing control or CD44 shRNAs at 28 days after cell injection (top panel); scale bar, 5 mm. The weight of tumors formed by HCT116 cells stably expressing the CD44 shRNA relative to that of those formed by the control cells was also determined at 28 days after cell injection (bottom panel). Data are mean ± SD for five animals in each group. *$p < 0.01$.

(B) Lysates of tumors formed by HCT116 cells stably expressing control or CD44 shRNAs were subjected to immunoblot analysis with indicated antibodies (right panel).

(C) Time course of the weight of tumors formed by HCT116 cells in nude mice treated with sulfasalazine (250 mg/kg) or saline. Data are mean ± SD for five mice per group. *$p < 0.01$ versus the corresponding value for saline-treated animals.

(D) Immunostaining of phospho-$p38^{MAPK}$ in tumors formed by HCT116 cells in nude mice treated with sulfasalazine or saline (left panels); the boxed regions are shown at higher magnification in the insets. Scale bars, 500 μm. Tumor lysates were also subjected to immunoblot analysis with indicated antibodies (right panel).

(E) The weight of tumors formed by HCT116 cells in nude mice treated with saline, CDDP (2 mg/kg), or CDDP (2 mg/kg) plus sulfasalazine (250 mg/kg) was determined at 28 days after cell injection. Data are mean ± SD for five animals per group. *$p < 0.01$.

(F) Model for regulation of ROS-$p38^{MAPK}$ signaling by CD44v. CD44v maintains a high-level GSH by stabilizing the expression of xCT at the plasma membrane of cancer cells. This action of CD44v results in suppression of ROS-$p38^{MAPK}$ signaling. HA, hyaluronic acid.

(G) Model for the role of the CD44v-xCT interaction in tumor development. CD44v and xCT interaction suppresses ROS-$p38^{MAPK}$ signaling in cancer cells by upregulating intracellular GSH, thereby promoting tumor development.

of CD44v (Ishimoto et al., 2010). We have now found that CD44v interacts with xCT and that CD44 ablation results in depletion of intracellular GSH and loss of cell surface expression of xCT, with the amount of CD98hc at the cell surface being apparently unaffected. Furthermore, forced expression of CD44v8–10, but not that of CD44s, accelerated the recovery of GSH content in $CD44^-$ cancer cells after GSH depletion induced by BSO. These observations suggest that CD44v-mediated stabilization of xCT at the plasma membrane promotes ROS resistance and maintenance of cancer cells.

xCT is a component of a plasma membrane transporter (the xc^- system) that mediates the cellular uptake of extracellular cystine in exchange for intracellular glutamate and thereby plays a key role in GSH synthesis. The activity of xCT-mediated cystine uptake in cancer cells is highly associated with cell proliferation, chemoresistance, and tumor growth (Gout et al., 2001; Lo et al., 2008). CD98hc is covalently linked to one of several light chains, including LAT1, LAT2, y+LAT1, y+LAT2, and ASC-1 in addition to xCT (Verrey et al., 2004), with the resulting complexes functioning as amino acid transporters at the plasma membrane. However, the precise mechanism by which CD98hc selects its binding partner to constitute the different types of amino acid transporter has remained unknown. In the present study we showed that CD44v stabilizes xCT expression at the plasma membrane, with the xc^- system then mediating cystine uptake and promoting GSH synthesis.

Another variant (exon 3-containing) isoform of CD44 has been shown to interact with monocarboxylate transporter (MCT)-1 and MCT-4, which are responsible for the transport of lactate in breast cancer cells (Slomiany et al., 2009). Therefore, it is possible that different CD44v isoforms contribute to the stabilization of several different types of transporter at the plasma membrane.

We previously showed that CD44 expressed in invasive cancer cells undergoes matrix metalloproteinase-dependent cleavage, which promotes turnover of CD44-mediated cell-matrix interaction and efficient invasion of extracellular matrix (Nagano et al., 2004; Nagano and Saya, 2004). These previous observations together with our present findings suggest that CD44 contributes to both the matrix invasion and ROS defense capabilities of cancer cells. It is possible that a switch between these dual functions of CD44 is determined by its stable expression at the cell surface or its cleavage.

Oxidative stress has been implicated in activation of both $p38^{MAPK}$ and p53-$p21^{CIP1/WAF1}$ signaling and, consequently, in cell-cycle arrest and senescence (Muller, 2009). Constitutive activation of $p38^{MAPK}$ has been shown to negatively regulate tumorigenesis (Bulavin et al., 2004; Dolado et al., 2007; Han and Sun, 2007). Furthermore, $p21^{CIP1/WAF1}$ is an important mediator of the differentiation of gastrointestinal epithelial cells (Katz et al., 2005; van de Wetering et al., 2002). Ablation of CD44 in mice harboring a transgene for tumor necrosis factor-α exacerbates chronic inflammatory arthritis as a result of excessive $p38^{MAPK}$ activation, indicative of increased levels of ROS (Hayer et al., 2005). Thus, expression of CD44 might be required to support cell proliferation in an inflammatory microenvironment characterized by increased oxidative stress. We have now shown that CD44 ablation suppressed gastric tumor growth in a mouse model of spontaneous tumorigenesis concomitant with the upregulation of $p38^{MAPK}$ phosphorylation and $p21^{CIP1/WAF1}$ gene expression. Furthermore, treatment with the specific xCT inhibitor sulfasalazine induced $p38^{MAPK}$ activation and suppressed CD44-dependent tumor growth in an HCT116 xenograft model. Furthermore, the effect of the ROS-inducing anticancer drug CDDP on CD44-dependent HCT116 tumor growth was significantly enhanced by sulfasalazine treatment. Together, these findings indicate that xCT-mediated suppression of ROS-$p38^{MAPK}$ signaling that negatively regulates the tumorigenic and proliferative capacities of tumor cells plays a role in the CD44-mediated expansion of tumor cells.

In conclusion our present data provide evidence that the expression of CD44v and its association with xCT block the ROS-induced stress signaling that results in growth arrest, cell differentiation, and senescence, and thereby promote the proliferation of cancer cells and the formation of lethal gastrointestinal tumors (Figures 8F and 8G). Given that CD44-expressing CSCs play a central role in resistance to cancer therapy, it has been suggested that definitive treatment should target the $CD44^{high}$ cell population in cancer. On the other hand, given that CD44 appears to have numerous functions, further investigation of other functions of this molecule in tumor growth and maintenance is warranted. Our present study indicates that CD44v-targeted therapy may impair the ROS defense ability of gastrointestinal cancer stem-like cells and thereby sensitize them to currently available cancer treatments.

EXPERIMENTAL PROCEDURES

Transgenic Mice

K19-Wnt1/C2mE transgenic (Gan) mice were described previously (Oshima et al., 2006). $CD44^{-/-}$ mice were obtained from The Jackson Laboratory (Bar Harbor, ME, USA). Gan mice were crossed with $CD44^{-/-}$ mice to generate $CD44^{-/-}$ Gan mice. Wild-type littermates of Gan mice were used as controls. All animal experiments were performed in accordance with protocols approved by the Ethics Committee of Keio University.

Statistical Analysis

Data are presented as mean ± SD and were analyzed with the unpaired Student's t test with the use of Excel 2007 (Microsoft, Redmond, WA, USA). A p value of <0.05 was considered statistically significant.

ACCESSION NUMBERS

Coordinates have been deposited in the GEO database with accession codes GSE20913, and GSE20914.

SUPPLEMENTAL INFORMATION

Supplemental Information includes six figures, one table, and Supplemental Experimental Procedures and can be found with this article online at doi:10.1016/j.ccr.2011.01.038.

ACKNOWLEDGMENTS

We thank I. Ishimatsu, N. Suzuki, Y. Ito, and M. Nakata for technical assistance; K. Arai for help in preparation of the manuscript; M. Fujiwara (Core Instrumentation Facility, Keio University School of Medicine) for assistance with microarray analysis; and S. Suzuki (Department of physiology, Keio University School of Medicine) for technical assistance with flow cytometric analysis. CE-MS analysis was performed by T. Matsu-ura, a technical assistant supported by the ERATO Gas Biology Project of the Japan Science and Technology Agency (JST). M.S. is the leader of the ERATO Gas Biology Project. This work was supported by grants from the Ministry of Education, Culture, Sports, Science, and Technology of Japan (to O.N. and H.S.) as well as in part by the "Academic Frontier" Project (2005–2007) and "Antiaging Center" Project (2008–2012) matching fund subsidies for private universities from the Ministry of Education, Culture, Sports, Science, and Technology and by the "A-STEP (Adaptable and Seamless Technology Transfer Program through R&D)" Project (2009–2011) matching fund subsidy from JST.

Received: March 12, 2010
Revised: July 29, 2010
Accepted: January 13, 2011
Published: March 14, 2011

REFERENCES

Al-Hajj, M., Wicha, M.S., Benito-Hernandez, A., Morrison, S.J., and Clarke, M.F. (2003). Prospective identification of tumorigenic breast cancer cells. Proc. Natl. Acad. Sci. USA *100*, 3983–3988.

Behl, C., Davis, J.B., Lesley, R., and Schubert, D. (1994). Hydrogen peroxide mediates amyloid beta protein toxicity. Cell *77*, 817–827.

Bulavin, D.V., Phillips, C., Nannenga, B., Timofeev, O., Donehower, L.A., Anderson, C.W., Appella, E., and Fornace, A.J., Jr. (2004). Inactivation of the Wip1 phosphatase inhibits mammary tumorigenesis through p38 MAPK-mediated activation of the p16(Ink4a)-p19(Arf) pathway. Nat. Genet. *36*, 343–350.

Chen, R.S., Song, Y.M., Zhou, Z.Y., Tong, T., Li, Y., Fu, M., Guo, X.L., Dong, L.J., He, X., Qiao, H.X., et al. (2009). Disruption of xCT inhibits cancer cell metastasis via the caveolin-1/beta-catenin pathway. Oncogene *28*, 599–609.

Collins, A.T., Berry, P.A., Hyde, C., Stower, M.J., and Maitland, N.J. (2005). Prospective identification of tumorigenic prostate cancer stem cells. Cancer Res. *65*, 10946–10951.

Dalerba, P., Dylla, S.J., Park, I.K., Liu, R., Wang, X., Cho, R.W., Hoey, T., Gurney, A., Huang, E.H., Simeone, D.M., et al. (2007). Phenotypic characterization of human colorectal cancer stem cells. Proc. Natl. Acad. Sci. USA *104*, 10158–10163.

Diehn, M., Cho, R.W., Lobo, N.A., Kalisky, T., Dorie, M.J., Kulp, A.N., Qian, D., Lam, J.S., Ailles, L.E., Wong, M., et al. (2009). Association of reactive oxygen species levels and radioresistance in cancer stem cells. Nature *458*, 780–783.

Dolado, I., Swat, A., Ajenjo, N., De Vita, G., Cuadrado, A., and Nebreda, A.R. (2007). p38alpha MAP kinase as a sensor of reactive oxygen species in tumorigenesis. Cancer Cell *11*, 191–205.

Dougherty, G.J., Landorp, P.M., Cooper, D.L., and Humphries, R.K. (1991). Molecular cloning of CD44R1 and CD44R2, two novel isoforms of the human CD44 lymphocyte "homing" receptor expressed by hemopoietic cells. J. Exp. Med. *174*, 1–5.

Gout, P.W., Buckley, A.R., Simms, C.R., and Bruchovsky, N. (2001). Sulfasalazine, a potent suppressor of lymphoma growth by inhibition of the x (c)- cystine transporter: a new action for an old drug. Leukemia *15*, 1633–1640.

Gunthert, U., Hofmann, M., Rudy, W., Reber, S., Zoller, M., Haussmann, I., Matzku, S., Wenzel, A., Ponta, H., and Herrlich, P. (1991). A new variant of glycoprotein CD44 confers metastatic potential to rat carcinoma cells. Cell *65*, 13–24.

Han, J., and Sun, P. (2007). The pathways to tumor suppression via route p38. Trends Biochem. Sci. *32*, 364–371.

Hayer, S., Steiner, G., Gortz, B., Reiter, E., Tohidast-Akrad, M., Amling, M., Hoffmann, O., Redlich, K., Zwerina, J., Skriner, K., et al. (2005). CD44 is a determinant of inflammatory bone loss. J. Exp. Med. *201*, 903–914.

Huang, Y., Dai, Z., Barbacioru, C., and Sadee, W. (2005). Cystine-glutamate transporter SLC7A11 in cancer chemosensitivity and chemoresistance. Cancer Res. *65*, 7446–7454.

Ishii, T., Sugita, Y., and Bannai, S. (1987). Regulation of glutathione levels in mouse spleen lymphocytes by transport of cysteine. J. Cell. Physiol. *133*, 330–336.

Ishimoto, T., Oshima, H., Oshima, M., Kai, K., Torii, R., Masuko, T., Baba, H., Saya, H., and Nagano, O. (2010). CD44(+) slow-cycling tumor cell expansion is triggered by cooperative actions of Wnt and prostaglandin E(2) in gastric tumorigenesis. Cancer Sci. *101*, 673–678.

Ito, K., Hirao, A., Arai, F., Takubo, K., Matsuoka, S., Miyamoto, K., Ohmura, M., Naka, K., Hosokawa, K., Ikeda, Y., and Suda, T. (2006). Reactive oxygen species act through p38 MAPK to limit the lifespan of hematopoietic stem cells. Nat. Med. *12*, 446–451.

Katz, J.P., Perreault, N., Goldstein, B.G., Actman, L., McNally, S.R., Silberg, D.G., Furth, E.E., and Kaestner, K.H. (2005). Loss of Klf4 in mice causes altered proliferation and differentiation and precancerous changes in the adult stomach. Gastroenterology *128*, 935–945.

Lo, M., Wang, Y.Z., and Gout, P.W. (2008). The x(c)- cystine/glutamate antiporter: a potential target for therapy of cancer and other diseases. J. Cell. Physiol. *215*, 593–602.

Muller, M. (2009). Cellular senescence: molecular mechanisms, in vivo significance, and redox considerations. Antioxid. Redox Signal. *11*, 59–98.

Nagano, O., and Saya, H. (2004). Mechanism and biological significance of CD44 cleavage. Cancer Sci. *95*, 930–935.

Nagano, O., Murakami, D., Hartmann, D., De Strooper, B., Saftig, P., Iwatsubo, T., Nakajima, M., Shinohara, M., and Saya, H. (2004). Cell-matrix interaction via CD44 is independently regulated by different metalloproteinases activated in response to extracellular Ca(2+) influx and PKC activation. J. Cell Biol. *165*, 893–902.

Oshima, H., Matsunaga, A., Fujimura, T., Tsukamoto, T., Taketo, M.M., and Oshima, M. (2006). Carcinogenesis in mouse stomach by simultaneous activation of the Wnt signaling and prostaglandin E2 pathway. Gastroenterology *131*, 1086–1095.

Owusu-Ansah, E., and Banerjee, U. (2009). Reactive oxygen species prime *Drosophila* haematopoietic progenitors for differentiation. Nature *461*, 537–541.

Phillips, T.M., McBride, W.H., and Pajonk, F. (2006). The response of CD24 (-/low)/CD44+ breast cancer-initiating cells to radiation. J. Natl. Cancer Inst. *98*, 1777–1785.

Ponta, H., Sherman, L., and Herrlich, P.A. (2003). CD44: from adhesion molecules to signalling regulators. Nat. Rev. Mol. Cell Biol. *4*, 33–45.

Sasaki, H., Sato, H., Kuriyama-Matsumura, K., Sato, K., Maebara, K., Wang, H., Tamba, M., Itoh, K., Yamamoto, M., and Bannai, S. (2002). Electrophile response element-mediated induction of the cystine/glutamate exchange transporter gene expression. J. Biol. Chem. *277*, 44765–44771.

Sato, H., Shiiya, A., Kimata, M., Maebara, K., Tamba, M., Sakakura, Y., Makino, N., Sugiyama, F., Yagami, K., Moriguchi, T., et al. (2005). Redox imbalance in cystine/glutamate transporter-deficient mice. J. Biol. Chem. *280*, 37423–37429.

Schmits, R., Filmus, J., Gerwin, N., Senaldi, G., Kiefer, F., Kundig, T., Wakeham, A., Shahinian, A., Catzavelos, C., Rak, J., et al. (1997). CD44 regulates hematopoietic progenitor distribution, granuloma formation, and tumorigenicity. Blood *90*, 2217–2233.

Shintani, T., Iwabuchi, T., Soga, T., Kato, Y., Yamamoto, T., Takano, N., Hishiki, T., Ueno, Y., Ikeda, S., Sakuragawa, T., et al. (2009). Cystathionine beta-synthase as a carbon monoxide-sensitive regulator of bile excretion. Hepatology *49*, 141–150.

Slomiany, M.G., Grass, G.D., Robertson, A.D., Yang, X.Y., Maria, B.L., Beeson, C., and Toole, B.P. (2009). Hyaluronan, CD44, and emmprin regulate lactate efflux and membrane localization of monocarboxylate transporters in human breast carcinoma cells. Cancer Res. *69*, 1293–1301.

Suematsu, M., Suzuki, H., Ishii, H., Kato, S., Yanagisawa, T., Asako, H., Suzuki, M., and Tsuchiya, M. (1992). Early midzonal oxidative stress preceding cell death in hypoperfused rat liver. Gastroenterology *103*, 994–1001.

Tanabe, K.K., Ellis, L.M., and Saya, H. (1993). Expression of CD44R1 adhesion molecule in colon carcinomas and metastases. Lancet *341*, 725–726.

Trachootham, D., Alexandre, J., and Huang, P. (2009). Targeting cancer cells by ROS-mediated mechanisms: a radical therapeutic approach? Nat. Rev. Drug Discov. *8*, 579–591.

van de Wetering, M., Sancho, E., Verweij, C., de Lau, W., Oving, I., Hurlstone, A., van der Horn, K., Batlle, E., Coudreuse, D., Haramis, A.P., et al. (2002). The beta-catenin/TCF-4 complex imposes a crypt progenitor phenotype on colorectal cancer cells. Cell *111*, 241–250.

Vermeulen, L., De Sousa, E.M.F., van der Heijden, M., Cameron, K., de Jong, J.H., Borovski, T., Tuynman, J.B., Todaro, M., Merz, C., Rodermond, H., et al. (2010). Wnt activity defines colon cancer stem cells and is regulated by the microenvironment. Nat. Cell Biol. *12*, 468–476.

Verrey, F., Closs, E.I., Wagner, C.A., Palacin, M., Endou, H., and Kanai, Y. (2004). CATs and HATs: the SLC7 family of amino acid transporters. Pflugers Arch. *447*, 532–542.

British Journal of Cancer (2011) 104, 300–307

www.bjcancer.com

Identification of HLA-A2-restricted CTL epitopes of a novel tumour-associated antigen, KIF20A, overexpressed in pancreatic cancer

K Imai[1,2], S Hirata[1], A Irie[1], S Senju[1], Y Ikuta[1,2], K Yokomine[1], M Harao[1,2], M Inoue[1,2], Y Tomita[1], T Tsunoda[3], H Nakagawa[3], Y Nakamura[3], H Baba[2] and Y Nishimura*[,1]

[1]Department of Immunogenetics, Graduate School of Medical Sciences, Kumamoto University, Kumamoto, Japan; [2]Department of Gastroenterological Surgery, Graduate School of Medical Sciences, Kumamoto University, Kumamoto, Japan; [3]Laboratory of Molecular Medicine, Human Genome Center, Institute of Medical Science, The University of Tokyo, Tokyo, Japan

BACKGROUND: Identification of tumour-associated antigens (TAAs) that induce cytotoxic T lymphocytes (CTLs) specific to cancer cells is critical for the development of anticancer immunotherapy. In this study, we aimed at identifying a novel TAA of pancreatic cancer for immunotherapy.

METHODS: On the basis of the genome-wide cDNA microarray analysis, we focused on KIF20A (also known as RAB6KIFL/MKlp2) as a candidate TAA in pancreatic cancer cells. The HLA-A2 (*A*02:01*)-restricted CTL epitopes of KIF20A were identified using HLA-A2 transgenic mice (Tgm) and the peptides were examined to check whether they could generate human CTLs exhibiting cytotoxic responses against KIF20A$^+$, HLA-A2$^+$ tumour cells *in vitro*.

RESULTS: *KIF20A* was overexpressed in pancreatic cancer and in some other malignancies, but not in their non-cancerous counterparts and many normal adult tissues. We found that KIF20A-2 (p12–20, LLSDDDVVV), KIF20A-8 (p809–817, CIAEQYHTV), and KIF20A-28 (p284–293, AQPDTAPLPV) peptides could induce HLA-A2-restricted CTLs in HLA-A2 Tgm without causing autoimmunity. Peptide-reactive human CTLs were generated from peripheral blood mononuclear cells of HLA-A2$^+$ healthy donors by *in vitro* stimulation with the three peptides, and those CTLs successfully exhibited cytotoxic responses to cancer cells expressing both KIF20A and HLA-A2.

CONCLUSION: KIF20A is a novel promising candidate for anticancer immunotherapeutic target for pancreatic cancers.

British Journal of Cancer (2011) **104,** 300–307. doi:10.1038/sj.bjc.6606052 www.bjcancer.com
Published online 21 December 2010

Keywords: anticancer immunotherapy; tumour-associated antigen; CTL; KIF20A/RAB6KIFL/MKlp2; HLA-transgenic mouse

Pancreatic cancer is one of the highly lethal malignancies with an overall 5-year survival rate of ~5% (Jemal *et al*, 2007). Although a surgical resection is the only treatment for long-term survival, patients with resectable pancreatic cancer are in the minority (9–22%) (Eloubeidi *et al*, 2006; Goonetilleke and Siriwardena, 2007). Furthermore, even the 5-year survival rate after a curative resection is reported to be ~20% (Cleary *et al*, 2004; Smeenk *et al*, 2005; Moon *et al*, 2006). Therefore, there is a strong need for development of novel therapeutic modalities.

Anticancer immunotherapy is considered to be the candidate modality for pancreatic cancer. Recently, analyses of gene expression profiles of cancer and normal cells using cDNA microarray technologies have provided an effective approach for the identification of tumour-associated antigens (TAAs) (Nakatsura *et al*, 2004b; Uchida *et al*, 2004; Yoshitake *et al*, 2004; Watanabe *et al*, 2005; Komori *et al*, 2006; Suda *et al*, 2006; Harao *et al*, 2008; Imai *et al*, 2008). This study analysed the gene expression profiles of pancreatic cancer using a genome-wide cDNA microarray consisting of 27 648 genes, which revealed that *KIF20A* was overexpressed in pancreatic cancer tissues but not in many normal tissues.

In this study, we examined whether KIF20A could be a potential target for anticancer immunotherapy. To this aim, human KIF20A-derived and HLA-A2-restricted cytotoxic T lymphocyte (CTL) epitopes were identified using HLA-A2 transgenic mice (Tgm), and the ability of peptides to induce KIF20A-reactive human CTLs that kill cancer cells and the safety not to induce autoimmune responses in the mouse were investigated.

MATERIALS AND METHODS

cDNA microarray analysis

A data set of genome-wide cDNA microarray analyses using cancerous and adjacent normal tissues obtained by a laser microbeam dissection (Nakamura *et al*, 2004) was used in this study. The tissue samples were obtained from surgical specimens

*Correspondence: Dr Y Nishimura;
E-mail: mxnishim@gpo.kumamoto-u.ac.jp
Revised 22 October 2010; accepted 16 November 2010; published online 21 December 2010

of pancreatic cancer patients. All patients provided their written informed consent to participate in this study.

Mice, cell lines, and HLA expression

The HLA-A2 Tgm, H-2D$^{b-/-}$ $\beta_2m^{-/-}$ double knockout mice introduced with a monochain gene construct of human β2m-HLA-A2.1(α1, α2)-H-2D^b(α3, transmembrane, and cytoplasmic) (Pascolo *et al*, 1997; Firat *et al*, 1999), were kindly provided by Dr FA Lemonnier. Mice were maintained and handled in accordance with the animal care guidelines of the Kumamoto University.

The human pancreatic cancer cell line PANC1, the colon cancer cell line CaCo-2, and a transporter associated with antigen processing (TAP)-deficient and HLA-A2 (*A*02:01*)-positive cell line T2 were purchased from the Riken Cell Bank (Tsukuba, Japan). The human liver cancer cell line SKHep1 and the human pancreatic cancer cell line PK9 were provided by Dr Kyogo Itoh (Kurume University, Kurume, Japan) and the Cell Resource Center for Biomedical Research Institute of Development, Aging and Cancer (Tohoku University, Sendai, Japan), respectively.

The expression of HLA-A2 was examined by flow cytometry with an anti-HLA-A2 monoclonal antibody (mAb), BB7.2 (One Lambda Inc., Canoga Park, CA, USA) to select HLA-A2-positive blood donors and target cancer cell lines.

Patients, blood samples, and tumour tissues

The clinical research using peripheral blood mononuclear cells (PBMCs) obtained from healthy donors was approved by the Institutional Review Board of the Kumamoto University. The cancer and adjacent non-cancerous tissues were obtained from 14 patients during routine diagnostic procedures from patients in the Kumamoto University Hospital. The tissues were subjected to either reverse transcription-PCR (RT-PCR) or immunohistochemical analyses as listed in Table 1. Blood and tissue samples were obtained from donors and patients, respectively, after receiving their written informed consent.

RT-PCR

Reverse transcription-PCR analyses were performed as described previously (Nakatsura *et al*, 2004a). The primers used were: *KIF20A*, sense 5′-CTACAAGCACCCAAGGACTCT-3′ (788-808, the 4th exon) and antisense 5′-AGATGGAGAAGCGAATGTTT-3′ (1400-1381, the 8th exon) and *ACTB*, sense 5′-CATCCACGAAACT ACCTTCAACT-3′ (903-925, the 5th exon) and antisense 5′-TCTCCTTAGAGAGAAGTGGGGTG-3′ (1535-1513, the 6th exon). Primer positions are shown according to cDNA sequences presented in the Gene Bank Accession numbers of NM_005733 for human *KIF20A* and of NM_001101 for human *ACTB*. The products were 612 bp long for *KIF20A* and 632 bp long for *ACTB*. After normalisation by the intensity for *ACTB* mRNA, the expression levels of *KIF20A* mRNA were compared among the tissues and cell lines.

Table 1 Expression of the *KIF20A* gene or protein in pancreatic cancer tissues

Patient	RT-PCR	IHC
1	−[a]	NT
2	−[a]	−
3	−[a]	−[b]
4	+[a]	NT
5	+[a]	+[b]
6	+[a]	+[b]
7	+[a]	NT
8	+[a]	NT
9	+[a]	+[b]
10	+[a]	NT
11	NT	+
12	NT	+
13	NT	+
14	NT	−

Abbreviations: IHC = immunohistochemical analysis; − = negative; NT = not tested; + = positive; RT-PCR = reverse transcription-PCR. [a]RT-PCR data are shown in Figure 2. [b]Immunohistochemical data are shown in Figure 3.

Western blot analysis and immunohistochemical examination

Western blot analysis and immunohistochemical staining of KIF20A using rabbit polyclonal anti-KIF20A antibody (category no. A300-879A) of Bethyl Laboratories (Montgomery, TX, USA) were performed as described previously (Nakatsura *et al*, 2001; Yoshitake *et al*, 2004). Immunohistochemical staining of CD4 or CD8 in tissue specimens of HLA-A2 Tgm immunised with the KIF20A-8$_{809-817}$ peptide was performed as described previously (Matsuyoshi *et al*, 2004).

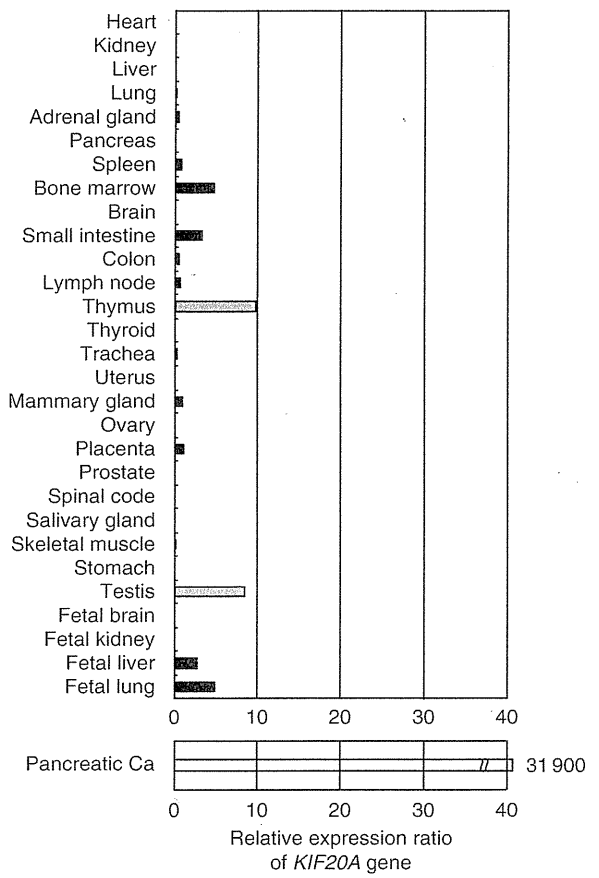

Figure 1 The relative expression ratio of *KIF20A* mRNA in pancreatic cancer tissues (Pancreatic Ca) and in various normal tissues based on a cDNA microarray analysis. The *KIF20A* gene was overexpressed in all six pancreatic cancer tissues investigated, but barely expressed in many normal tissues, except for in the testis and thymus. The ratio of relative expression levels of *KIF20A* mRNA in six pancreatic cancer tissues to that of disease-free counterparts was calculated. For normal tissues, the average expression level of *KIF20A* mRNA in all tissues was assigned to be 1.0, and the relative expression level of *KIF20A* mRNA in each tissue was calculated. For pancreatic cancer, the expression levels of *KIF20A* mRNA in adjacent normal pancreatic tissues were assigned to be 1.0, and the relative expression levels of *KIF20A* mRNA in pancreatic cancers were calculated using specimens obtained from six patients with pancreatic cancer.

Lentiviral gene transfer

KIF20A cDNA was transduced into SKHep1 cells by a lentiviral vector-mediated gene transfer as described previously (Tahara-Hanaoka *et al*, 2002; Irie *et al*, 2006). The expression of KIF20A was confirmed by western blot analysis.

Table 2 Expression of the *KIF20A* gene in pancreatic cancer and various malignancies investigated by cDNA microarray analyses[a]

	N	Positive rate[a] (%)	Average of relative expression ratio
Pancreatic cancer	6/6	100	31 900
Small cell lung cancer	15/15	100	22
Bladder cancer	30/31	97	20 500
Non-small cell lung cancer	20/22	91	25 800
Cholangiocellular carcinoma	7/11	64	3 780
Breast cancer	29/61	44	322
Prostate cancer	11/36	31	4
Renal cell carcinoma	3/11	27	5
Oesophageal cancer	2/13	15	3
Colorectal cancer	2/31	3	2
Gastric cancer	0/4	0	0

Data are obtained from our previous studies (Nakao *et al*, 1995; Uchida *et al*, 2004; Yoshitake *et al*, 2004; Taniuchi *et al*, 2005; Watanabe *et al*, 2005). [a]The relative expression ratio was calculated by dividing the value of the expression of *KIF20A* mRNA in cancer cells by that in the normal counterpart, and a relative expression ratio (cancer/normal tissue) of >5 was considered to be positive.

Induction and response of KIF20A-reactive mouse CTLs

A total of 36 human KIF20A-derived peptides (purity >95%) with predicted high binding scores for HLA-A2 (*A*02:01*) by BIMAS software (NIH, Bethesda, MD, USA; http://www-bimas.cit.nih.gov/) were synthesised by the American Peptide Company (Sunnyvale, CA, USA; Supplementary Table 1). The HLA-A2 Tgm were immunised intraperitoneally twice on days 0 and 7 with bone marrow-derived dendritic cells (BM-DCs) pulsed with 12 sets of a mixture of 3 kinds of the 36 synthesised peptides. Seven days after the last immunisation, CD4-depleted spleen cells ($CD4^-$ spleen cells) from Tgm using CD4 microbeads (Miltenyi Biotec, Auburn, CA, USA) were stimulated *in vitro* with BM-DCs pulsed with each peptide. The CTL responses to the peptides were tested by the ELISPOT assay (human INF-γ ELISPOT kit, BD Biosciences, Franklin Lakes, NJ, USA).

Induction of KIF20A-reactive human CTLs

Peripheral monocyte-derived DCs were generated from $CD14^+$ cells isolated from PBMCs of HLA-A2-positive healthy donors using CD14 microbeads (Miltenyi Biotec), with stimulation of 100 ng ml^{-1} granulocyte/macrophage colony-stimulating factor, 10 ng ml^{-1} interleukin (IL)-4, and Streptococcal OK-432 (Picibanil, Chugai Pharmaceutical Co., Ltd., Tokyo, Japan) (Naito *et al*, 2006) as described previously (Harao *et al*, 2008). The cells were morphologically changed to express many dendrites, and their expression levels of MHC class-II and CD80 were upregulated after the stimulation with OK-432. The DCs were pulsed with 20 μg ml^{-1} candidate peptides in the presence of 4 μg ml^{-1} β2-microglobulin

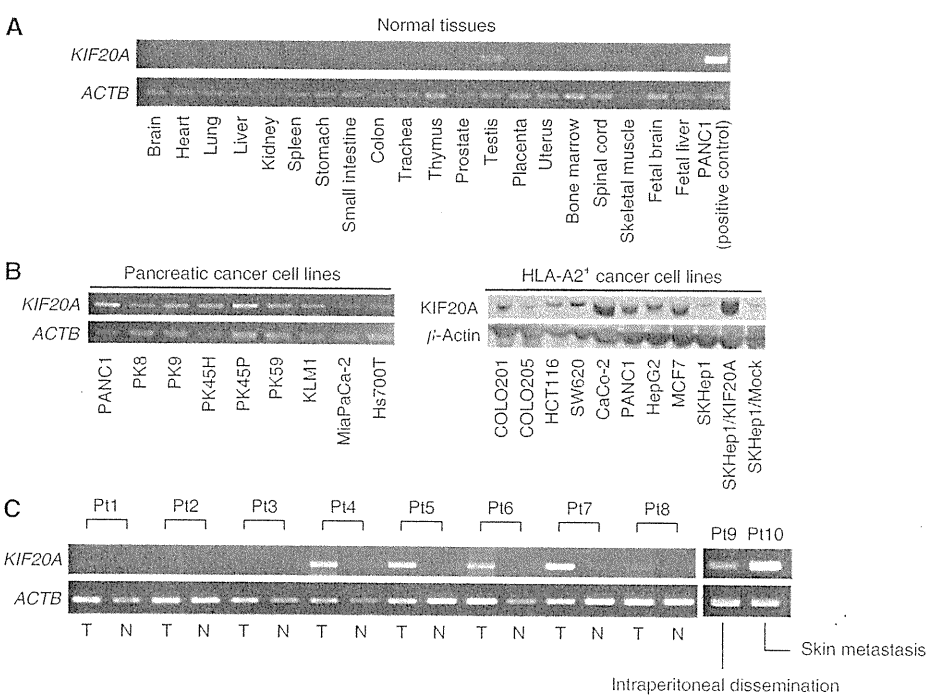

Figure 2 Expression of *KIF20A* mRNA and protein in human normal tissues, cancer cell lines, and pancreatic cancer tissues. (**A**) RT–PCR analysis of *KIF20A* mRNA expression in various normal tissues. *KIF20A* mRNA was not detected except for faint expression observed in the testis. (**B**) The expression of *KIF20A* mRNA and protein in various cancer cell lines investigated by RT–PCR (left) and western blot analyses (right). *KIF20A* mRNA was detected in all pancreatic cancer cell lines examined. The major bands at ~100 kDa, which corresponds to the calculated molecular weight for KIF20A, are shown. It must be noted that SKHep1 and SKHep1/Mock expressed only a trace amount of the KIF20A protein, whereas *KIF20A* cDNA-transfected SKHep1, SKHep1/KIF20A, relatively expressed a large amount of the protein. (**C**) RT–PCR analyses of the *KIF20A* expression in pancreatic cancer tissues (T), and their normal counterparts (N). The expression of the *KIF20A* mRNA was detected in five of eight pancreatic tumour tissues, but little expression was detected in their normal counterparts. It must be noted that *KIF20A* mRNA expression was also detected in the peritoneum (patient 9 (Pt9)) and metastatic foci of the skin (patient 10 (Pt10)).

(Sigma-Aldrich, St Louis, MO, USA) for 2 h at 37°C in AIM-V medium (Invitrogen, Carlsbad, CA, USA) containing 2% autologous plasma. The DCs were then irradiated (40 Gy) and incubated with $CD8^+$ cells isolated from the same PBMCs using CD8 microbeads (Miltenyi Biotec). These cultures were set up in 24-well plates; each well contained 1×10^5 peptide-pulsed DCs, 2×10^6 $CD8^+$ T cells, and 5 ng ml^{-1} human IL-7 (Wako, Osaka, Japan), in 2 ml AIM-V with 2% autologous plasma. After 2 days, these cultures were supplemented with human IL-2 (PeproTec, Rocky Hill, NJ, USA) to a final concentration of 20 IU ml^{-1}. Two additional stimulations with peptide-loaded autologous DCs were carried out on days 7 and 14. Six days after the last stimulation, antigen-specific CTL responses were investigated by the ELISPOT assay and the ^{51}Cr release assay as described previously (Komori *et al*, 2006).

CTL responses against cancer cell lines

Human CTLs were co-cultured with cancer cells or peptide-pulsed T2 cells as a target (5×10^3 per well) at the indicated effector/target ratio, and a standard ^{51}Cr release assay was performed (Komori *et al*, 2006). An HLA-A2 (*A*02:01*)-binding HIV-derived peptide, SLYNTVATL, was used as an irrelevant control peptide (Parker *et al*, 1992). Blocking of HLA-class I or HLA-DR in the ELISPOT assay was performed as follows: the target cancer cells were incubated with 10 μg ml^{-1} anti-HLA-class I mAb, W6/32, or 10 μg ml^{-1} anti-HLA-DR mAb, H-DR-1 (kindly provided by Dr Kyogo Itoh (Nakao *et al*, 1995)) for 1 h before co-culture with CTLs, and the inhibitory effects of mAbs on the production of IFN-γ by CTLs were monitored (Gomi *et al*, 1999).

RESULTS

Identification of the *KIF20A* gene upregulated in pancreatic cancer and various malignancies based on cDNA microarray analyses

Using genome-wide cDNA microarray analyses, it turned out that six genes, namely *CDH3*, *KIF20A*, *MICAL2*, *TRIM29*, *ABHD*, and *EPHA4*, were overexpressed in the six pancreatic cancer tissues in comparison with their adjacent normal counterparts, and we reported that CDH3/P-cadherin is a new TAA for immunotherapy of pancreatic, gastric, and colorectal cancers (Imai *et al*, 2008). In this study, we focused on *KIF20A* as another pancreatic cancer-specific TAA for immunotherapeutic target. The cDNA microarray analyses revealed that expression of the *KIF20A* gene in pancreatic cancer tissues was markedly enhanced in all six patients investigated (the average of the relative expression ratio: 31 900, ranging 15–72 000), whereas the *KIF20A* gene was faintly expressed only in the testis and thymus among normal tissues (Figure 1). In addition, overexpression of the *KIF20A* gene was also observed in other malignancies, such as lung and bladder cancers (Table 2) (Kitahara *et al*, 2001; Hasegawa *et al*, 2002; Kikuchi *et al*, 2003; Nakamura *et al*, 2004; Obama *et al*, 2005) .

Expression of *KIF20A* mRNA and protein in normal organs, cancer cell lines, and pancreatic cancer tissues

The expression of the *KIF20A* gene in normal tissues was analysed by RT–PCR analyses, which revealed its exclusive expression in the testis and thymus (Figure 2A). On the other hand, the expression of the *KIF20A* gene was detected in almost all

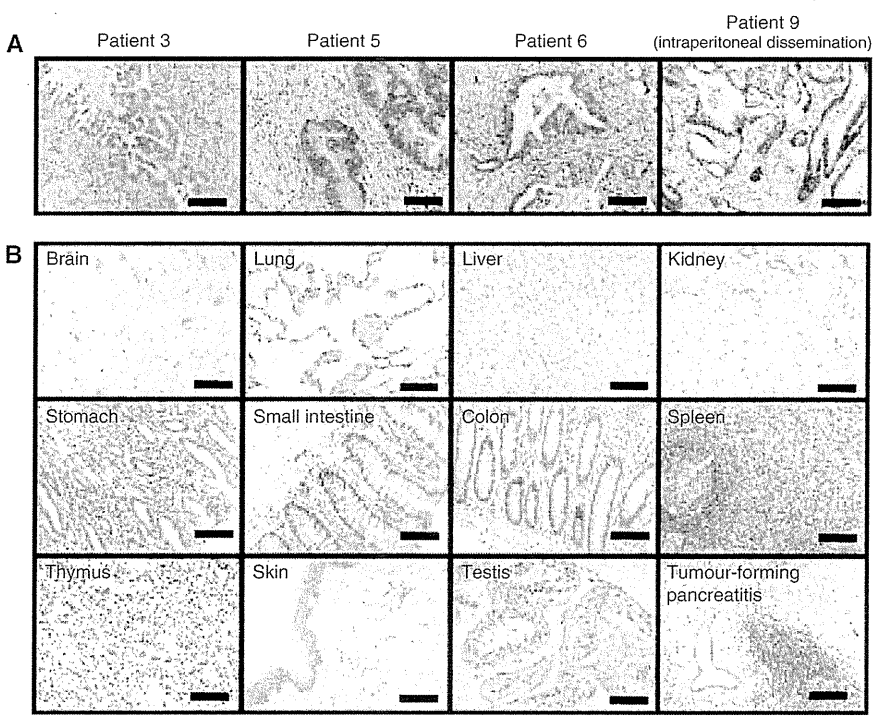

Figure 3 Immunohistochemical analyses of the KIF20A protein in (**A**) pancreatic cancer and in (**B**) various normal tissues. (Panel **A**) A strong staining of KIF20A was mainly observed at the cytoplasm and nuclei of cancer cells in six of nine cases (representative patients 5, 6, and 9 are shown), whereas a very weak staining was observed in acinar cells and in the normal ductal epithelium of their normal adjacent pancreatic tissues. A pancreatic cancer tissue without KIF20A expression is also shown (Patient 3). A similar strong staining was observed in the metastatic foci of the peritoneum (Patient 9). (Panel **B**) KIF20A was not detected in the normal brain, lung, liver, kidney, stomach, small intestine, colon, spleen, skeletal muscle, skin, thymus, and testis. Little staining was detected in tumour-forming pancreatitis. Positive staining signals are seen as brown. The scale bars represent 100 μm.

pancreatic and other HLA-A2-positive cancer cell lines tested (Figure 2B, left). Those observations essentially coincided with data obtained by cDNA microarray analyses.

We then checked the expression of the *KIF20A* gene in surgically resected pancreatic cancer tissues and their adjacent normal counterparts by RT-PCR analyses. The *KIF20A* gene was detected in five of eight pancreatic cancer tissues, whereas virtually no expression was observed in their normal counterparts (Figure 2C). It is noteworthy that *KIF20A* was also detected in the metastatic foci of the skin and peritoneum.

Western blot analysis revealed expression of the KIF20A protein in various HLA-A2$^+$ cancer cell lines tested, except for SKHep1 (Figure 2B, right). To confirm the tumour-associated overexpression of the KIF20A protein, various paraffin-embedded normal tissue specimens and pancreatic cancer specimens were examined by immunohistochemical analyses. We investigated nine samples of pancreatic cancer (Table 1), and a strong staining of KIF20A was mainly observed in the cytoplasm and nuclei of cancer cells in six cases, whereas a very weak staining was observed in acinar cells and the normal ductal epithelium of their normal adjacent pancreatic tissues (Figure 3A). Little staining was detected in tumour-forming pancreatitis. KIF20A was not detected in the normal brain, lung, liver, kidney, stomach, small intestine, colon, spleen, skeletal muscle, skin, thymus, and skin (Figure 3B). Therefore, the pattern of KIF20A protein expression essentially paralleled with its gene expression profile.

Identification of KIF20A-derived and HLA-A2-restricted mouse CTL epitopes using HLA-A2 Tgm

A total of 36 peptides with high binding scores to HLA-A2 (*A*02:01*) by BIMAS (Supplementary Table 1) were immunised to HLA-A2 Tgm, and CD4$^-$ spleen cells were stimulated *in vitro* with BM-DCs pulsed with each peptide. The CD4$^-$ spleen cells stimulated with KIF20A-2 (p12-20, LLSDDDVVV), KIF20A-8 (p809-817, CIAEQYHTV), and KIF20A-28 (p284-293, AQPDTAPLPV) peptides produced a significant amount of INF-γ in a peptide-specific manner in the ELISPOT assay (Figure 4A). Those CD4$^-$ spleen cells (2×10^4) showed 149.0 ± 22.2, 117.2 ± 23.4, and 141.2 ± 5.5 spot counts per well in response to BM-DCs pulsed with the KIF20A-2, KIF20A-8, and KIF20A-28 peptides, respectively, whereas they showed 32.6 ± 9.9, 51.4 ± 7.8, and 19.2 ± 5.2 spot counts per well, respectively, without peptide loading ($P<0.01$). No significant peptide-specific response was observed with the other peptides. These results suggest that the KIF20A-2, KIF20A-8, and KIF20A-28 peptides could be the HLA-A2-restricted CTL epitope peptides in HLA-A2 Tgm and those peptides were expected to be epitopes for human CTLs.

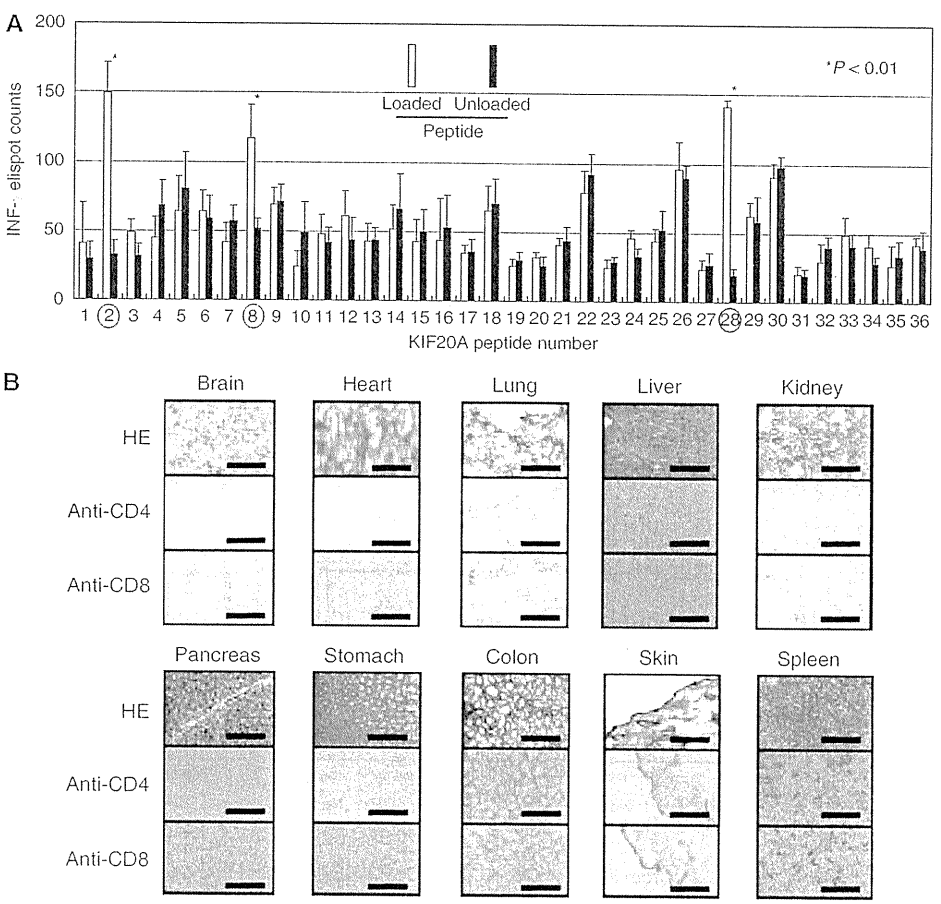

Figure 4 Identification of HLA-A2-restricted mouse CTL epitopes of human KIF20A using HLA-A2 Tgm. (**A**) HLA-A2 Tgm were immunised with syngeneic BM-DCs pulsed with the peptide mixtures as described in the 'Materials and Methods' section, and CD4$^-$ spleen cells were stimulated with BM-DCs pulsed with or without each peptide for 6 days. INF-γ-producing CTLs were detected by an ELISPOT assay. KIF20A-2 (LLSDDDVVV), KIF20A-8 (CIAEQYHTV), and KIF20A-28 (AQPDTAPLPV) peptides indicated by the circles were shown to induce peptide-reactive CTLs. These assays were performed twice with similar results. (**B**) Immunohistochemical staining with anti-CD4 or anti-CD8 mAb in tissue specimens of HLA-A2 Tgm immunised with the KIF20A-8 peptide. After two-times vaccinations, these specimens were removed and analysed.

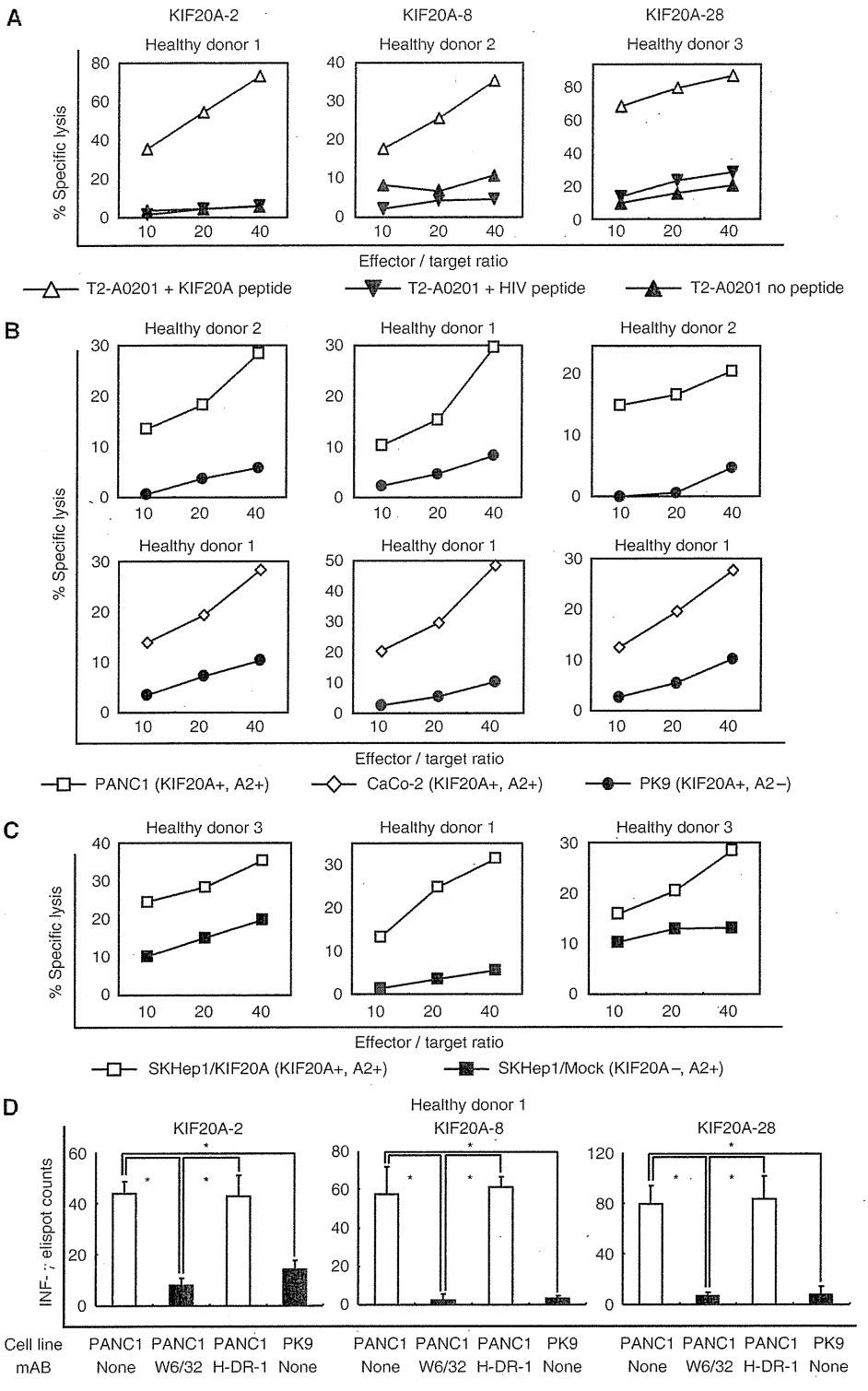

Figure 5 Induction of KIF20A-specific human CTLs from PBMCs of three HLA-A2-positive healthy donors. (**A**) KIF20A peptide-reactive CTLs generated from PBMCs of three HLA-A2-positive healthy donors effectively killed T2 cells (HLA-A2$^+$, TAP deficient) pulsed with each peptide but not those unpulsed or pulsed with irrelevant and HLA-A2-restricted CTL epitopes of HIV. (**B**) Human CTLs exhibited cytotoxicity to the KIF20A$^+$, HLA-A2$^+$ human pancreatic cancer cell line PANC1 and to the colon cancer cell line CaCo-2, but not to KIF20A$^+$, HLA-A2$^-$ human pancreatic cancer cell line PK9. (**C**) The cytotoxicity of human CTLs was KIF20A specific. Those CTLs killed SKHep1/KIF20A, but not mock-transfected SKHep1 cells. Representative data are shown. (**D**) Human CTL responses were inhibited by anti-HLA-class I mAb (W6/32, IgG_{2a}) but not by anti-HLA-DR mAb (H-DR-1, IgG_{2a}). The target cells used were PANC-1cell (KIF20A$^+$, HLA-A2$^+$) and PK9 cell (KIF20A$^+$, HLA-A2$^-$). (Panels **A**–**D**) Representative data from one of the three donors with similar results are shown.